Technische Universität München
TUM School of Medicine and Health

Human acute microelectrode array recordings with broad cortical access, single-unit resolution, and parallel behavioral monitoring

Viktor Maria Eisenkolb

Vollständiger Abdruck der von der TUM School of Medicine and Health der Technischen Universität München zur Erlangung eines

Doktors der Medizinischen Wissenschaft (Dr. med. sci.)

genehmigten Dissertation.

Vorsitz: Prof. Dr. Angelika Harbauer

Prüfer der Dissertation:

1. Prof. Dr. Simon Nikolas Jacob
2. apl. Prof. Dr. Jens Gempt

Die Dissertation wurde am 16.10.2023 bei der Technischen Universität München eingereicht und durch die TUM School of Medicine and Health am 10.04.2024 angenommen.

Table of contents

1 INTRODUCTION ..... - 1 -

1.1 RECORDINGS OF NEURONAL ACTIVITY *IN VIVO* ..... - 2 -
1.1.1 ELECTROPHYSIOLOGICAL RECORDING METHODS ..... - 2 -
1.1.2 IMAGING TECHNIQUES OF NEURONAL ACTIVITY IN VIVO ..... - 5 -
1.1.3 UNTAPPED POTENTIAL OF AWAKE NEUROSURGERY FOR FUNDAMENTAL SCIENCE ..... - 6 -
1.2 WORKING MEMORY ..... - 7 -
1.2.1 THE FRONTO-PARIETAL NETWORK ..... - 7 -
1.2.2 DIFFERENTIATION BETWEEN BEHAVIORALLY RELEVANT AND IRRELEVANT INFORMATION ..... - 8 -
1.3. NUMBER CODING ..... - 9 -

2 MATERIALS AND METHODS ..... - 10 -

2.1 ETHICS APPROVAL ..... - 10 -
2.2 TECHNICAL EQUIPMENT ..... - 10 -
2.2.1 ELECTROPHYSIOLOGY SETUP ..... - 10 -
2.2.2 ELECTRODE ARRAYS ..... - 11 -
2.2.3 BEHAVIORAL TASK AND MONITORING ..... - 13 -
2.2.4 FURTHER EQUIPMENT ..... - 13 -
2.3 SUBJECTS ..... - 13 -
2.4 WORKING MEMORY TASK ..... - 15 -
2.5 MEA IMPLANTATION AND INTRAOPERATIVE EXTRACELLULAR RECORDINGS ..... - 16 -
2.6 SPIKE SORTING ..... - 19 -
2.7 ANALYSIS OF THE LFPS ..... - 19 -
2.7.1 PREPROCESSING ..... - 19 -
2.7.2 SPECTRAL TRANSFORMATION ..... - 20 -
2.7.3 POWER ..... - 20 -
2.7.4 SPIKE TRIGGERED AVERAGE OF THE LFP ..... - 20 -

3 RESULTS ..... - 21 -

3.1 SUCCESSFULLY COMPLETION OF WORKING MEMORY TASK DURING AC ..... - 21 -
3.1.1 EXAMPLE OF DEVIATION: ACALCULIA ..... - 23 -
3.2 BROAD CORTICAL ACCESS ..... - 24 -
3.2.1 REACHING A LARGE PART OF THE LEFT HEMISPHERE DURING AWAKE SURGERY ..... - 25 -
3.3 LOW DAMAGE AT INSERTION SITE ..... - 26 -
3.4 TEMPERATURE OF THE EXPOSED CORTICAL SURFACE DECREASES ONLY SLIGHTLY DURING TUMOR RESECTION. - 26 -
3.5 STABLE WIDE-BAND EXTRACELLULAR RECORDINGS DURING AWAKE CRANIOTOMY ..... - 28 -
3.5.1 LOCAL FIELD POTENTIALS ..... - 28 -
3.5.2 EXTRACTION OF ACTION POTENTIALS AS SINGLE- AND MULTI-UNIT ACTIVITY ..... - 30 -
3.6 EXPLOITING THE TWO-DIMENSIONAL STRUCTURE OF THE ELECTRODE ARRAY ..... - 33 -
3.7. CODING OF NONSYMBOLIC AND SYMBOLIC NUMBERS ..... - 35 -

4 DISCUSSION ..... - 37 -

4.1 MEAs IN NEUROSURGICAL CRANIOTOMIES – INCORPORATING FUNDAMENTAL SCIENCE INTO THE OPERATING ROOM ..... - 37 -
4.2 FEASIBILITY OF PERFORMING A TASK ADDRESSING HIGHER HUMAN COGNITIVE FUNCTIONS DURING AWAKE CRANIOTOMY ..... - 38 -
4.3 MEAs ARE SUITABLE FOR ACUTE RECORDINGS OF HUMAN BRAIN ACTIVITY ..... - 39 -
4.4 GRID-LIKE ELECTRODE ARRANGEMENT ..... - 40 -
4.5 GEOMETRIC CONFIGURATION OF THE MEA IS DECISIVE FACTOR OF SNR ..... - 40 -
4.6 COMBINATION OF IN VIVO WITH IN VITRO EXPERIMENTS ..... - 41 -
4.7 ETHICAL ISSUES AND EXPERIMENTAL LIMITATIONS ..... - 41 -

5 REFERENCES ..... - 43 -

6. ACKNOWLEDGEMENTS ..... - 50 -

List of abbreviations

AC	Awake craniotomy
AG	Angular gyrus
BCI	Brain computer interface
ECoG	Electrocorticogram
EEG	Electroencephalogram
fMRI	Functional MRI
IPC	Inferior parietal cortex
IPS	Intraparietal sulcus
LFP	Local field potential
lPFC	Lateral prefrontal cortex
MEA	Multi electrode array
MEP	Motor evoked potentials
MFG	Middle frontal gyrus
NSA	Neural signal amplifier
NSP	Neural signal processor
PCG	Postcentral gyrus
PET	Positron emission tomograph
PFC	Prefrontal cortex
SFG	Superior frontal gyrus
SMG	Supramarginal gyrus
SSEP	Somatosensory evoked potentials
VEP	Visually evoked potentials
WM	Working memory

1 Introduction

The human brain has been subject to research for a long time. After failures of individual brain areas caused by malformation, trauma or other disease entities and the associated consequences for the behavior of the individual, specific functions could be assigned to these macroscopic areas long before the era of modern science. For example, the isolated damage to the frontal brain of the American railroad worker Phineas P. Gage in 1848 caused by an accident helped physicians of the time to better understand the importance of the frontal lobe for personality and executive control. The symptom complex experienced by this patient is now referred to as frontal lobe disorder (Niedermeyer 1998). The autopsy of an aphasic patient, whose speech comprehension functioned perfectly but who could only produce the syllable “Tan”, and the evidence of a neurosyphilitic lesion in the patient’s left inferior frontal gyrus in 1861 made it possible to assign this brain region (“Broca’s area”) to the higher cognitive function of speech production (Pearce 2009).

Great advances followed with the discovery of neurons and the transmission of information through electrical activity. Nevertheless, the interaction of individual neurons and their functioning neuronal networks in the human brain are still not understood in many parts. This is partly due to the still limited access to the human brain in the awake state for invasive measurements. Neuronal activity in higher cognitive functions can only be imaged in awake humans, yet only in very special situations, such as awake craniotomies, direct access to the brain is possible. One of these situations is awake surgery of the human brain during tumor resections. To date, there are only a few established methods for recording the activity of individual neurons or networks in the acute setting that achieve sufficient signal quality.

The main goal of my graduate work was to establish techniques to implant high-density, multi-channel microelectrode arrays into functional parts of the left prefrontal and posterior parietal cortex of awake neurosurgical patients undergoing resection of left-hemispheric brain masses. These acute, large-scale extracellular recordings were combined with cognitive tasks requiring e.g., the categorization of abstract numerical information.

In the following, I will provide information about neuronal activity measurement and working memory and give an overview of currently used methods in the field highlighting their advantages and limitations. Ultimately, this work aims to show why our approach opens up new possibilities to study species-independent principles of cognitive functioning and to address neuronal mechanisms that govern human-specific cognition on a microcircuit level.

This work is based on a recently published article (Eisenkolb, Held et al. 2023).

1.1 Recordings of neuronal activity *in vivo*

Due to their complexity, neuronal networks still raise many questions, especially regarding higher cognitive functions. In contrast to other methods for measuring neuronal activity in living objects, the biophysiological basis of the generation of electrical signals in the extracellular medium of the brain is largely understood.

All processes of neuronal activity in a certain brain volume and thus each transmembrane current leads to an intracellular and extracellular voltage deviation, which form a measurable superimposed field (local field potential, LFP) measured in Volts, with respect to a reference location. What the LFP derived at a particular point ultimately looks like is defined by the manifold contributions of the various sources in the brain. Factors such as the magnitude of the currents, the spatial situation at the location of their origin and the temporal coordination are critical (Herreras 2016). Accordingly, the neuronal geometry and cortical architecture at the recording site also influence the extracellular field.

As described above, there are hence different events that contribute to the formation of the extracellular signal to varying degrees. Synaptic activity, high-frequency action potentials, which will later be referred to as spiking activity, Ca^{2+}-mediated spikes and intrinsic currents are just a few examples of the mechanisms that contribute to this.

Several cell types contribute differently to the extracellular field due to their distinct abilities to generate a dipole. A pyramidal cell for example can generate a strong dipole along the somatodendritic axis due to its structure (R 1947). Accordingly, the arrangement of the cells is decisive for the strength of the extracellular field. In the cortex, the apical dendrites of neighboring pyramidal cells lie parallel to each other. This enhances the summation of the individual dipoles and is one of the reasons why the LFPs of the cortex are larger compared to those of most deeper-seated brain areas (Linden, Tetzlaff et al. 2011).

1.1.1 Electrophysiological recording methods

There are many different methods to record the activity of the human central nervous system. They differ, for example, in terms of target volume, invasiveness, cost, and clinical feasibility, but logically also in their usability in various contexts. A selection of these is presented below.

1.1.1.1 Electroencephalography

One of the oldest and most used methods in neurological clinical and scientific settings is electroencephalography (EEG). The signals, which are usually derived with electrodes distributed over the subject's head in a wide variety of configurations, are still standard in the diagnosis of various diseases, first and foremost epilepsy, despite the great advances in imaging. Since it is relatively easy

and quick to perform and inexpensive, it is used in multiple contexts. Thus, the EEG is also increasingly applied outside of classical neurological diagnostics, e.g., EEG-based depth of anesthesia monitoring (Hajat, Ahmad et al. 2017) or EEG-based neurofeedback training (Bu, Young et al. 2019). In addition to the noninvasive surface recordings described so far, there are various forms of invasive, intracranial EEG that are only used for very specific issues where noninvasive means have been fully exhausted (Reif, Strzelczyk et al. 2016).

1.1.1.2 Electrocorticography

However, neuronal signals can also be measured using a more invasive method directly from the brains surface: electrocorticography (ECoG). Transferred from animal experiments to humans at the beginning of the 20th century (Jung and Berger 1979), ECoG serves as a tool in medical diagnostics and science due to its higher amplitude (Hill, Gupta et al. 2012) and local resolution compared to scalp EEG. The electrodes can be put either directly on the cortex (under the dura, subdural) or on top of the dura (epidural). A widespread application is modern neurosurgery. For instance, in tumor resections near critical areas such as the central region, ECoG strip electrodes are used for intraoperative control of motor/sensory evoked potentials to increase the postoperative outcome of patients. In addition to the acute setting, ECoG has also been used to permanently transmit signals after chronic implantations (Miller, Hermes et al. 2020). Together with the exponential growth in computing power in recent years, this opens innumerous possibilities for the generation of brain-computer interfaces.

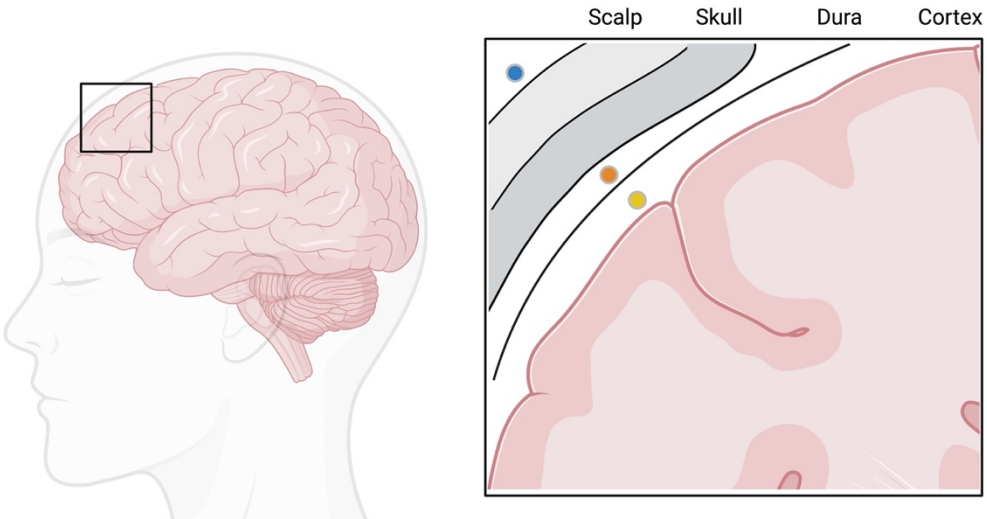

Fig 1 *Schematic drawing of different locations of EEG recordings. Blue: scalp EEG. Orange; epidural EEG. Yellow: subdural EEG.*

1.1.1.3 Evoked potentials

Evoked potentials are critical in assessing the excitability of the central and peripheral parts of the human nervous system. They are measured as electrical activity in response to an external stimulus. Motor (MEP), somatosensory (SSEP), brainstem auditory and visually evoked potentials (VEP) are used daily in clinical practice as a diagnostic measure of central and peripheral nerve damage of various causes. In newborns, auditory evoked potentials can confirm the integrity of the auditory pathway (Habib and Habib 2021). In neurosurgical interventions, intraoperative neuromonitoring with measurement of evoked potentials is regularly used to identify eloquent areas or to detect iatrogenic damage to relevant pathways at an early stage (Wong, Shils et al. 2022).

MEP recording can be combined with transcranial magnetic stimulation to perform functional mapping, for instance before neurosurgery.

1.1.1.4 Intracortical measurements

Extracellular neuronal activity can also be measured intracortically. Since the first single-unit recordings in the live human brain in 1955 (Ward and Thomas 1955), implantable electrodes have been continuously developed and their range of application in medicine and research expanded. Unlike the other ways of signal derivation, they have the advantage of not summing the signal from thousands or millions of neurons and can reach deep-lying neuronal structures (Buzsaki, Anastassiou et al. 2012) (Kaiju, Doi et al. 2017). In the clinical setting, macroelectrodes located in deeper brain areas are used for instance in the treatment for Parkinson's disease (Deuschl, Schade-Brittinger et al. 2006), epilepsy (Osorio, Frei et al. 2005) or depression (Mayberg, Lozano et al. 2005). In addition, implantable microelectrodes are gaining importance in basic or clinical research. As computing power increases, new hardware manufacturing capabilities emerge and our understanding of neural networks improves, hopes grow for functional brain-machine interfaces. For this, stable and high-resolution recordings of single units and LFPs are crucial. Recent milestones include the movement of a prosthetic limb (Hochberg, Bacher et al. 2012) or achievement speech synthesis (Willett, Avansino et al. 2021, Willett, Kunz et al. 2023).

Considering the large number of different applications and the resulting different requirements for the electrodes, there is not one solution for all issues (Wang, Yang et al. 2023). Depending of the focus of the specific implanted electrode, the design ranges from single electrodes or rigid multielectrode arrays (Maynard, Nordhausen et al. 1997) to flexible electrode threads which can be spatially implanted as required (Musk and Neuralink 2019, Chung, Sellers et al. 2022, Paulk, Kfir et al. 2022).

Materials, implantation methods, connectors: there is vast potential for improvement. However, it is clear that reliable recordings of action potentials from humans are possible – the basic prerequisite for further development and for the translation of experiments from animal models to humans.

1.1.1.5 Patch clamp technique (intracellular measurements)

Since its discovery, the Nobel Prize-winning patch clamp technique has allowed us to examine, at a cellular level, processes such as signaling, secretion, and synaptic transmission by providing a high-resolution method of observing the function of individual ionic channels in a variety of normal and pathological cell types (Liem, Simard et al. 1995). After preparation, the outer cell membrane is brought into contact with a thinly extended glass pipette filled with a conductive solution and an electrode. The experimental setup makes it possible to measure the conductivity through the ion channels of the section of the membrane (Neher and Sakmann 1976).

1.1.2 Imaging techniques of neuronal activity in vivo

Neuronal activity cannot only be objectified by directly measuring electrical activity. There are several imaging modalities that are used in research and clinical application.

1.1.2.1 Functional magnetic resonance imaging

Functional magnetic resonance imaging (fMRI) is a widely used tool due to its non-invasiveness. In fMRI, imaging of anatomical structures is combined with temporally and spatially resolved measurement of activity of the imaged structures. "Activity" is objectified by changes in tissue perfusion, blood volume changes or oxygen concentration (Logothetis 2008). This can be combined with the processing of tasks by subjects in the clinical or scientific setting. Besides the quasi-ubiquitous availability, this may be one of the reasons for its popularity. By indirectly mapping electrical activity by measuring primarily hemodynamic changes, the limitations of this method concerning temporal or spatial resolution for example, become apparent (Glover 2011).

1.1.2.2 PET

Another imaging modality standardly used worldwide to image the brain in clinical and scientific settings is positron emission tomography (PET). A positron-emitting radiopharmaceutical is introduced into the body. The emitted positron unites with an electron and produces two photons (γ-ray) which travel in opposite directions (Lameka K, Ichise M. Handb Clin Neurol. 2016). As the PET scanners have coincidence γ-ray detectors to detect the pair as it is hitting opposite detectors at the same time, the positron annihilation can be assumed to have happened on the connecting line between these two detectors. Thus, a 3D image of these events can be created. This modality allows us to, for example, visualize processes in the field of metabolism, amino acid transport and vascularization in the brain.

Frequent combination with CT or MRI scans additionally provides accurate representation of the anatomy.

However, the understanding of the function of individual neurons or the basis of the interplay of neuronal networks is not possible, but the importance in the diagnosis of neurodegenerative or tumor disease is growing.

1.1.3 Untapped potential of awake neurosurgery for fundamental science

Awake craniotomies (AC) are a valuable tool in modern neurosurgery since it allows specialists to monitor eloquent brain functions and perform real-time mapping of the brain during an intervention. For glioma surgery, this mapping is primarily performed by the neurosurgeon with a handheld probe or by the placement of a subdural grid or strip electrode (Gerritsen, Broekman et al. 2022).

It was shown that AC with brain mapping is a safe method to maximally remove supratentorial lesions with minimal postoperative neurological deficits (Sacko, Lauwers-Cances et al. 2011, Chacko, Thomas et al. 2013). This is particularly advantageous for tumors located in eloquent areas where significant limitations in the patient's quality of life can be expected in the case of iatrogenic damage. Speech, as one of the abilities that – in contrast to motor or sensory abilities – cannot be measured otherwise during general anesthesia, has a special role in this regard. As anomia and speech production errors during surgery are indicators of the patient's postoperative status in both short- and long-term outcome, AC emerged as the gold standard for glioma resections in eloquent areas (Collee, Vincent et al. 2022). In practice, this is objectified by permanently checking speech production and comprehension through observation or the processing of specific tasks by the patient with the help of medical personnel trained for this purpose.

Contrary to what is frequently assumed by laypersons or professionals outside the field, AC is well tolerated by the patients and does not cause significant psychological trauma (Starowicz-Filip, Prochwicz et al. 2022).

The time required for an AC, a factor that cannot be disregarded in a modern clinic, is similar to the time required for a comparable operation under general anesthesia (Brown, Shah et al. 2013).

Because of the expected heterogeneity between surgeons and centers as well as the dependence on patient performance, the key variables as well as the factors leading to the indication of ACs continue to be evaluated.

Besides its clinical relevance, the setting of AC provides an almost unique opportunity for scientists of the human brain: It offers broad cortical access while allowing task processing by an awake subject.

1.2 Working memory

To generate behavior that goes beyond the simple principle of action and reaction, one needs a means of short-term storage for processing information. This platform is called working memory (WM) and is the prerequisite for goal-directed behavior (Chatham and Badre 2015, Miller, Lundqvist et al. 2018). It can be described as temporary storage and manipulation of critical information for complex cognitive tasks as language comprehension, learning and reasoning (Baddeley 1992). In contrast to long-term memory in which information is stored and recalled at a later point in time, the information in working memory remains in an accessible state for a limited period (Cowan 2017).

The way in which this storage functions at the neuronal level has long been the subject of debate. Data generated in non-human primates several decades ago showed that there is a plateau-like persistent activity (increased firing rates in the absence of sensory stimulation at the single cell level during the delay phase of a working memory task in higher-order association cortex (Fuster and Alexander 1971, Funahashi, Bruce et al. 1989). These cortices include in particular the prefrontal cortex as well as parietal cortex (Miller and Cohen 2001, Lara and Wallis 2015).

This delay-activity is characterized by increased spiking rates during a short period of time – a previously presented stimulus must be remembered for a few seconds before a specific action is required by the subject of a task for example (Miller, Erickson et al. 1996, Pasternak and Greenlee 2005).

In addition to the change in spiking activity, specific patterns in the LFPs were also identified. Oscillatory activity i.e., synchronized activity, in the alpha, beta, gamma, and theta bands was detected during working memory tasks (Honkanen, Rouhinen et al. 2015, Lundqvist, Rose et al. 2016, Jacob, Hahnke et al. 2018). This indicates that working-memory information is represented by synchronized activity across higher-order cortices as the fronto-parietal network (Salazar, Dotson et al. 2012).

1.2.1 The fronto-parietal network

Where is the information stored in WM? It was shown that the altered activity in PFC during the delay period did, inter alia, encode stimulus information (Curtis and D'Esposito 2003, Riggall and Postle 2012). This stimulus related information could also be demonstrated in posterior sensory areas (Ester, Serences et al. 2009, Emrich, Riggall et al. 2013).

One of the theories therefore attributes a mediating role to the PFC within the network (Lara and Wallis 2015). This is supported, for example, by a study in which monkeys with lesions in the lateral prefrontal cortex (lPFC) had poorer performance in a delayed match-to-sample task, suggesting that lPFC plays a role in attending to stimuli and accessing motion information stored in other areas (Pasternak, Lui et al. 2015).

There is ample evidence that other involved areas are sensory cortices, as already described above. There has been detection of WM related activity in visual (Miller, Li et al. 1993), gustatory (Lara, Kennerley et al. 2009) and auditory (Gottlieb, Vaadia et al. 1989) cortex.

As mentioned in the previous subsection, one of the mechanisms of interaction between the PFC and the sensory areas is oscillatory activity. In a study, the phase locking value, a measure quantifying the synchrony between theta oscillations in primary visual cortex and PFC of monkeys performing a visual WM task, was significantly increased in successful trials (Liebe, Hoerzer et al. 2012). Since then, these results have been confirmed (Daume, Gruber et al. 2017). Furthermore, it has been shown that in the parallel frequency-specific interaction of frontal and parietal cortices lie mechanisms of WM information coding and of protection of this information against interference (Jacob, Hahnke et al. 2018).

An interpretation of this is that the stimulus information remains within the sensory cortices and that the PFC has the role of focusing the individual's attention on and select the relevant input to perform the executive functions needed to control correct cognitive processing of the information (Postle 2006).

Due to the partly different methods used in studying the animal and human brain, the transferability of some of the results is controversially discussed. It therefore seems even more important to develop ways to obtain the needed data from the human brain.

1.2.2 Differentiation between behaviorally relevant and irrelevant information

The brain is flooded with countless stimuli every second. In order to gain cognitive control over one's actions, important information must be distinguished from unimportant information (Baddeley 2012). This is critical as working memory has a limited capacity (Luck and Vogel 1997, Cowan 2001). This capacity appears to be similar between species (Cowan 2001, Buschman, Siegel et al. 2011, Balakhonov and Rose 2017).

Studies suggest that in the setting of processing a visual working memory task, specialized neurons in posterior parietal cortex (PPC) represent the last stimulus shown – irrelevant of whether it was a distractor or not (Constantinidis and Steinmetz 1996, Feredoes, Heinen et al. 2011).

In monkeys and humans with lesioned lPFC, the ability to filter information according to importance is impaired (Chao and Knight 1995, Chao and Knight 1998, Suzuki and Gottlieb 2013), which therefore implies the involvement of the PFC in these gating mechanisms.

According to the current state of knowledge, there are two simultaneously applied strategies for this purpose. First, distracting information might be suppressed or averted by filtering attention of the subject (Lennert and Martinez-Trujillo 2011, Suzuki and Gottlieb 2013). Second, distractor information can be bypassed by retaining and restoring target information (Jacob and Nieder 2014).

1.3. Number coding

An important content for the behavior of living beings, which must be stored in working memory, is number. Numbers are an abstract concept and can be multiplied, for example, in accordance with the rules of arithmetic. These considerations are based on more or less complex decision making, which is why number coding is an approach for neuroscientists to explore mechanisms of cognitive control (Nieder 2016).

There are multiple reasons why, according to the current state of science, a non-verbal quantification system common to humans and animals is assumed. Animals of different species, i.e., birds, fish or insects, use set size (numerosity) for their decision making (Gross, Pahl et al. 2009, Agrillo, Piffer et al. 2011, Soto and Wasserman 2014). Toddlers can distinguish the number of objects (Siegler and Opfer 2003) and adults can estimate the number of objects that have not been presented long enough to count (Whalen 1999). This “approximate number system” is a non-verbal quantification system common to both the animal kingdom and humans. In human childhood, initially meaningless verbal expressions and shapes (later digits) are linked to numerical ideas. This human verbal number is the basis for counting and developing superior mathematical skills (Nieder and Dehaene 2009).

In the hierarchy of the neural number network, the lPFC and the intraparietal sulcus (IPS) are placed high. In these two regions number neurons, i.e., single cells that respond most strongly to their preferred number, have been detected in various experiments in non-human primates (Nieder, Freedman et al. 2002, Nieder and Miller 2003). To our knowledge, the encoding of these number neurons happens in an abstract way across modalities (e.g. visual vs auditory) which points to a *sense of number* common to animals and humans (Dehaene, Dehaene-Lambertz et al. 1998, Arrighi, Togoli et al. 2014). In this context, it is worth mentioning that these processes also occur in untrained animals and number neurons are thus not an “acquired” entity or skill (Viswanathan and Nieder 2013).

Another hypothesis that was also tested is whether symbolic (Arabic numerals) and non-symbolic number is processed in the same or at least a similar way. It was found that IPS activity is sensitive to numerosity regardless of format, but the encoding is different, as clear behavioral differences between trials with different number formats were found (Fias, Lammertyn et al. 2003, Piazza, Pinel et al. 2007, Eger, Michel et al. 2009, Lyons, Ansari et al. 2015, Kutter, Bostroem et al. 2018).

By simultaneously testing verbal and non-verbal number coding in humans in a working memory task, the fundaments of higher cognitive functions in humans can be better understood. How do associations cortices respond at the single unit level during number procession in the working memory? Differences in the response behavior of individual cells or networks in the human brain are to be expected here und should therefore be further investigated.

2 Materials and methods

2.1 Ethics approval

The study was conducted in accordance with the Declaration of Helsinki and approved by the institutional review board (Ethikkommission der Fakultät für Medizin der Technischen Universität München, Ismaninger Straße 22, 81675 Munich, Germany; 528/15 S). Prior to inclusion in the study all subjects provided written informed consent to participate.

2.2 Technical equipment

2.2.1 Electrophysiology setup

For the recording of neuronal signals in the intraoperative setting, the *NeuroPort Biopotential Signal Processing system* (NSP, Blackrock Neurotech, Salt Lake City, USA) was used. The signals from the electrode array were forwarded to the *Neural Signal Amplifier* (NSA) via a *Patient cable*. Here, the analog signal undergoes amplification, filtering and digitization. In order to transmit it via a fiber optic cable to the NSP, it is additionally converted into the optical domain. Thus, the signal is protected against electromagnetic interference from this step on.

In a later phase of our study (P10-P13), Blackrock's *CerePlex E* and a digital hub was used instead of the patient cable and the NSA. The *CerePlex E* is a digital headstage which is directly connected to the pedestal. It digitizes the signal at the skull and hence provides better protection against noise. Settings for signal amplification, filtering and digitization were identical in both setups (1^{st}-order Butterworth high-pass at 0.3 Hz and 3^{rd}-order Butterworth low-pass at 7.5kHz, sampling rate 30 kHz, 16-bit resolution). The NSP also receives the digital codes for monitoring the patient's behavior.

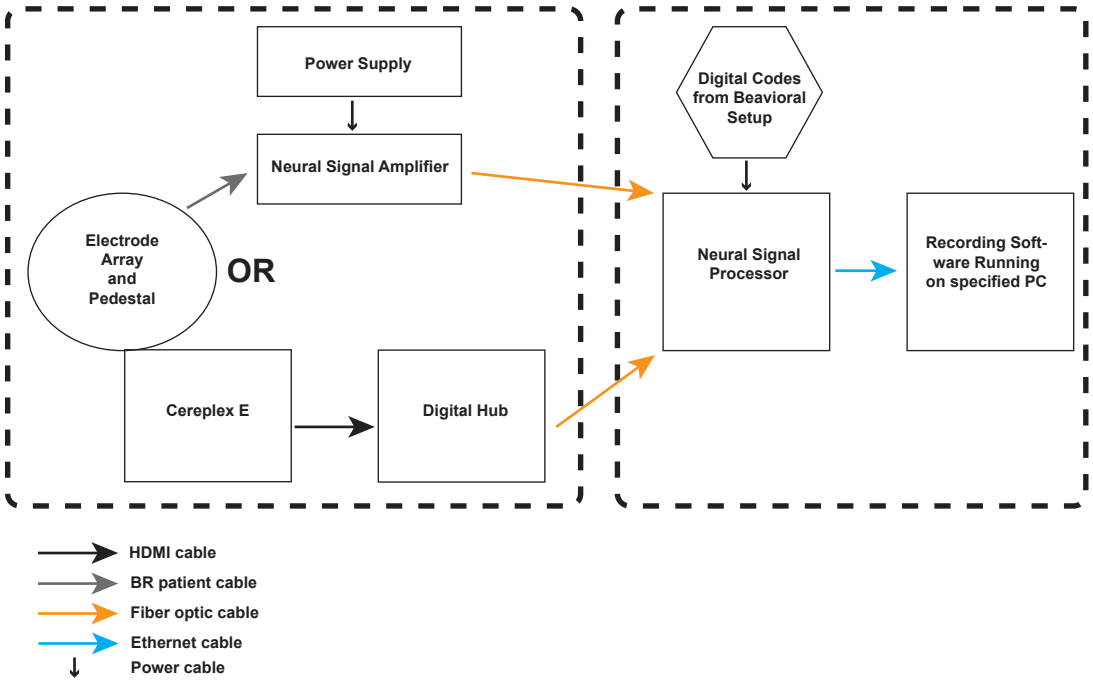

Figure 2. *Setup used for the intraoperative recordings during awake craniotomies; adapted from Blackrock Neurotech NeuroPort Manual.*

Attached to the MEA were two reference wires. Technically, it was possible to switch between the two. Due to the high-quality reference signals on both in all recordings, this was not necessary.

2.2.2 Electrode arrays

One *NeuroPort Array IrOx* planar multielectrode array (MEA; Blackrock Neurotech) was used per patient, also known as "Utah Array". This is a multielectrode array with 96 contacts configured in a 4x4mm 10x10 grid, which can record the activity of single units (neurons), multi-units as well as local field potentials (LFP). The electrode length was 1.5mm and the metallization was done with iridium oxide. Two contacts, that can be used for referencing, lead directly into the pedestal, which is screwed onto the skull as described later.

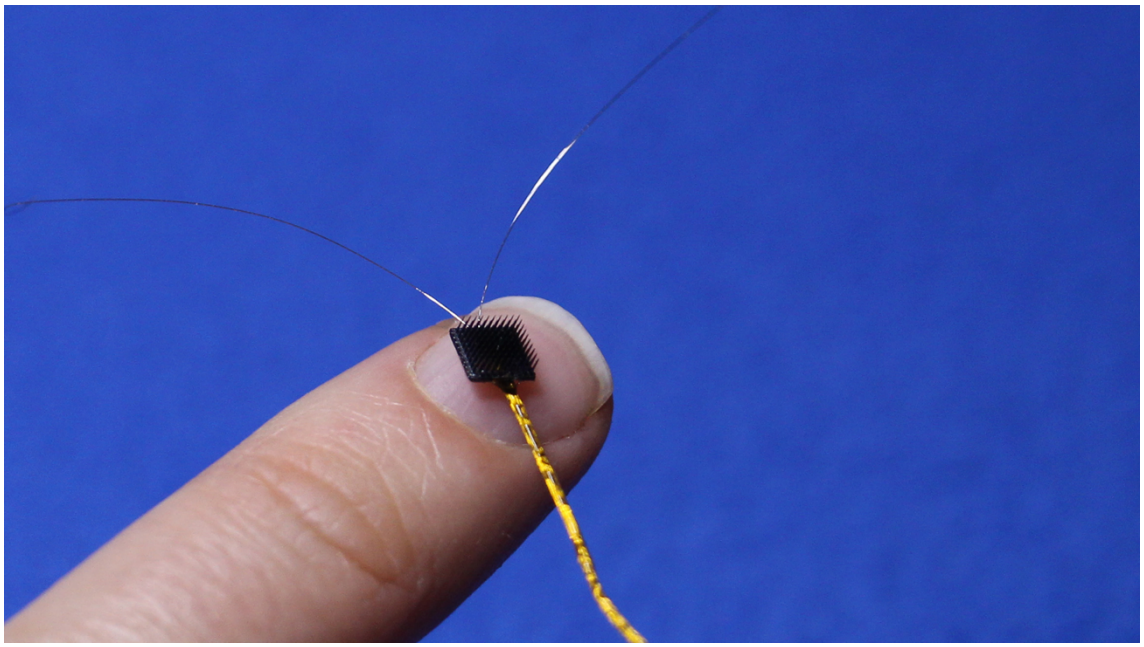

Figure 3. *Utah electrode Array with its 100 microelectrodes that are arranged in a 10 by 10 grid. The distance of each electrode from the horizontal and vertical neighboring electrodes is 400µm.*

A modified version of the array (Fig 4) was also used in which every second row of contacts was removed with a laser by the manufacturer. This doubled the distance between the contacts from 400µm to 800µm and reduced the number of contacts to 25.

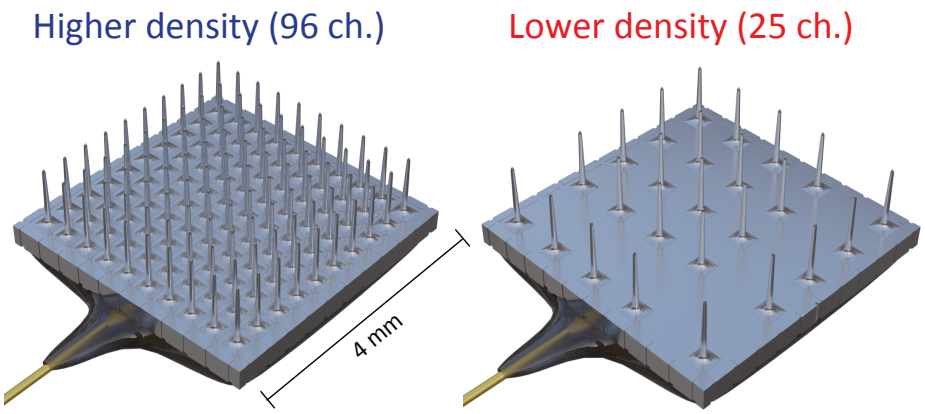

Figure 4. *Computer-aided design (CAD) drawings of the standard higher-density MEA (left, 96 active channels) and of the custom lower-density MEA (right, 25 active channels) used for intraoperative recordings.*

The electrodes were implanted with the pneumatic *NeuroPort Electrode Array Inserter* which was connected to the isolating transformator *polyMIT 700* (Sedlbauer, Grafenau, Germany) for safety reasons in the potentially wet environment of the operating room.

2.2.3 Behavioral task and monitoring

For the intraoperative processing of the task by the patients, we used the software *MonkeyLogic* (Asaad and Eskandar 2008) and its second version *MonkeyLogic 2* (Hwang, Mitz et al. 2019) in combination with a *Dell Optiplex 3050* (Dell Technologies Inc., Round Rock, USA), which was equipped with the *NI PCIe-6321 DAQ Card* (National Instruments, Austin, USA). A *12-inch monitor* (Beetronics B.V., Nieuwegein, Netherlands) was used to display visual stimuli to the patients to complete the task. Their response was given via a *manual switch for medical use* (Merz Medizintechnik, Metzingen, Germany).

2.2.4 Further equipment

The thermal imaging camera used to measure temperatures of the exposed cortical surface during surgery was the *FLIR T1030SC* (Sensor GmbH, Mönchengladbach, Germany).

2.3 Subjects

The study was conducted on 13 patients, 4 women and 9 men (see Table 1) with intracerebral tumors. All of them were scheduled for resection of a left-hemispheric space-occupying lesion, mainly glioblastomas, by the Department of Neurosurgery on short notice. The timing and execution of the treatment was not altered except for the implantation of the array.

A group of patients (P01-P03) was implanted with the unmodified electrode array, which was then explanted after a short period of time with a hem of cortical tissue measuring less than 1mm for histological examination. Since no electrophysiological measurements were performed during these surgeries, these patients were not awake craniotomized and therefore under general anesthesia.

At an early stage, two patients (P04-P05) were implanted with a 96-channel MEA but remained anesthetized during electrophysiological recordings.

The third group of eight patients (P06-P13) was implanted with either a 96-channel or modified 25-channel electrode array during the resection of a left-hemispheric tumor when awake. This was not randomized but happened sequentially. The median age of this group at the time of surgery was 58

years, the mean was 58,125 years. Among them were two females and six males. All of them were right-handed, but two of them used their left hand for the response of the task due to minor physical restrictions or personal preference. Five of them underwent the procedure under antiepileptic medication. All subjects spoke German as their first language.

ID	Sex	Age	Tumor location	Procedure	State	Array location	Chan-nels	Spikes	Single units (Multi units)	Behavior	Notes
P01	F	68	right frontal	histology	anesthetized	IPC	96				
P02	M	54	right parietal	histology	anesthetized	IPC	96				
P03	M	62	right parietal	histology	anesthetized	IPC	96				
P04	M	56	left frontal	setup testing and recording	anesthetized	MFG	96	no	0 (0)		
P05	F	75	left central	setup testing and recording	anesthetized	SFG	96	no	0 (0)		
P06	M	57	left parietal	recording	awake	AG/SMG	96	(yes)	7 (5)	number task	
P07	M	73	left parietal	recording	awake	AG/SMG	96	no	0 (0)	number task	performance in non-symbolic trials ↓
P08	F	55	left parietal	recording	awake	IPC	96				No data acquisition, bad ground
P09	M	51	left fronto-parietal	recording	awake	MFG	96	no	0 (0)	number task	performance in non-symbolic trials ↓
P10	M	32	left temporal	recording	awake	SMG/AG	25	yes	32 (25)	number task	
P11	M	67	left frontal	recording	awake	SMG/AG	25	yes	18 (14)	number task	
P12	M	71	left insular	recording	awake	AG/SMG	25				no data acquisition intraop. complication unrelated to implantation
P13	F	59	left central	recording	awake	SMG/PCG	25	yes	N/A (N/A)	number task	spiking activity as in P10 and P11 prior to sudden SNR drop

Table 1: *Study participants*

The site of implantation was reconstructed for each patient (see Table 1 and Fig 5). For this purpose, we used the intraoperative neuronavigation, preoperative MRI-datasets and photographic documentation. We implanted in locations that were planned preoperatively: 3 of them in the frontal cortex, 10 in the parietal cortex. The exact anatomical location was reconstructed using the steps described in the methods, three three-dimensional examples are shown in Figure 12.

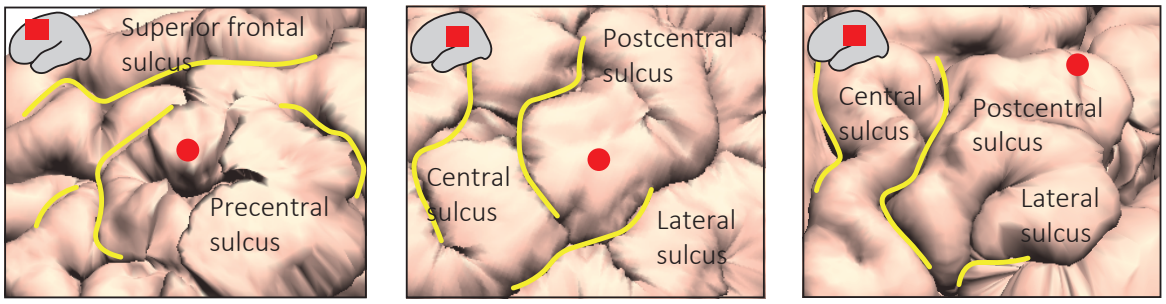

P04: middle frontal gyrus (p = 0.78)

P10: supramarginal gyrus (p = 0.50)

P06: angular gyrus (p = 0.50)

Figure 5. *Cortical surface reconstructions of the implantation site in three example participants. The probability of implantation in the specified gyrus is given according to the JuBrain probabilistic cytoarchitectonic map. Red dots depict the site of implantation. Yellow lines highlight sulci.*

For reconstructing the electrode implantation sites and the craniotomies, a combination of *SPM12* (Wellcome Center Human Neuroimaging), BrainSuite (Shattuck and Leahy 2002), the *Julich-Brain atlas* (Katrin Amunts 2020), the *ICBM template brain* (Mazziotta, Toga et al. 2001) and custom-written Matlab code.

2.4 Working memory task

The subjects performed a modified version of a delayed match-to-numerosity task performed by macaques in earlier experiments (Andreas Nieder 2002). The patients were placed 40 to 50 cm in front of a black screen. Since the head was fixed in a skull clamp according to neurosurgical standards during the entire operation, the patient screen was attached to a monitor arm adjustable in all planes and thus set up at a distance of 40-50 cm for optimal processing of the task stimuli by each individual subject. At the beginning of each trial, a white circle appeared as a fixation point in the middle of the screen. As soon as the patient pressed the hand switch held in the preferred hand, a larger gray circle was displayed for 500 ms (=fixation/pre-sample period). Then, a number from two to four or six to eight appeared for 150 ms inside the boundaries of the gray circle (= sample). This numerosity was represented either by black dots arranged randomly within the gray circle or in the form of an Arabic numeral (Arial, 40-56 pt).

The participants were required to memorize the sample number for 1,000 ms and compare it to the number of dots (in nonsymbolic trials) or the Arabic numeral (in symbolic trials) presented in a 1,000 ms test stimulus. If the quantities matched (50% of trials), participants released the button (correct Match trial). If the quantities were different (50% of trials), the participants continued to push the

button until the matching quantity was presented in the subsequent image (correct non-match trial). Match and non-match trials and nonsymbolic and symbolic trials were pseudo-randomly intermixed. New stimuli were generated for each participant and recording.

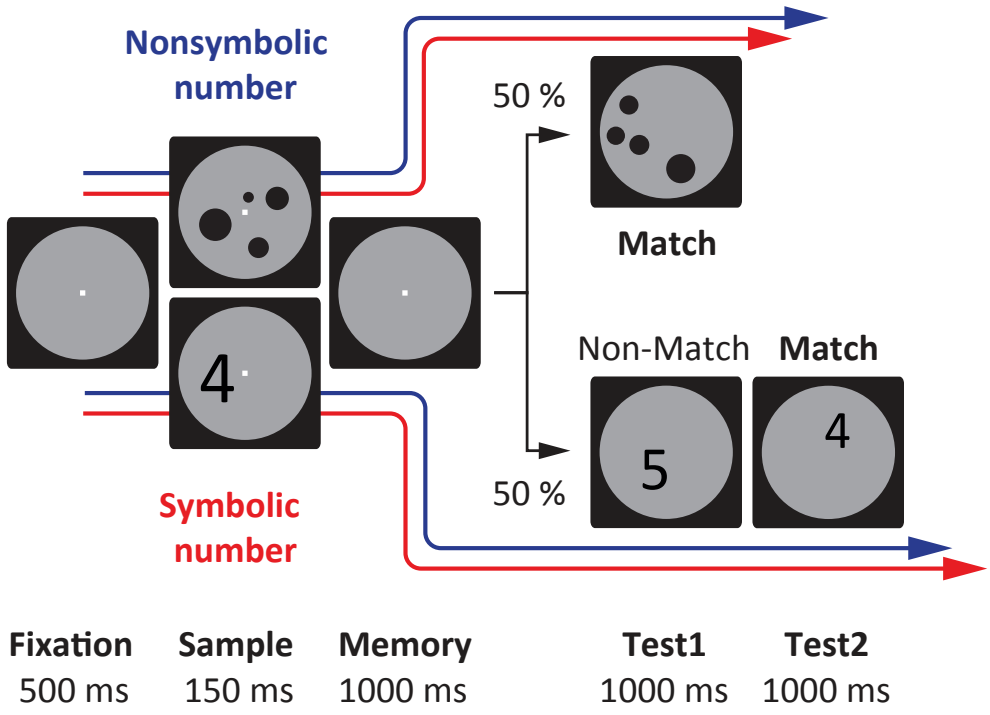

Figure 6. *Delayed-match-to-number task. Participants memorized the number of the sample stimulus and compared it with a subsequently presented test number. Trials were presented either in nonsymbolic notation (sets of dots, numerosities) or in symbolic notation (Arabic numerals).*

Custom-written Matlab code (Mathworks, Natick, USA) was used for the evaluation of the behavioral data.

2.5 MEA implantation and intraoperative extracellular recordings

The subjects underwent MRI imaging for planning and interactive 3D navigation for image-guided surgery and determination of the electrode implantation site. Physical examinations and speech tests were performed by the department for neurosurgery to exclude the possibility of preoperative impairments that would stand in the way of our study. Minor speech or motor impairments, past epileptic seizures or mildly reduced vision did not lead to exclusion.

One week to one day before the surgery, the task was explained to the patients. They performed a limited amount of training trials until they understood the structure of the task and completed it

satisfactorily. Otherwise, the patients were prepared and premedicated as for a regular awake craniotomy.

On the day of the surgery, anesthetic induction was performed. After the craniotomy was achieved and the dura was opened, the electrode array was implanted at the previously determined location. The preoperatively planned implantation sites were located using MRI-guided neuronavigation (Brainlab, Germany). To avoid injury to prominent vascular structures, in some cases the implantation site was deviated by a few millimeters from previously defined on the cross-sectional image.

The implantation was done with one short impulse (20 psi at 3.5 ms) perpendicular to the cortex with a pneumatic inserter wand on the surface of the array following the manufacturer's guidelines (Blackrock Neurotech). The use of a dedicated external wand holder was considered to be inconvenient, as this unnecessarily prolongs the implantation process. The wand was secured manually. The wand touched the array's dorsal pad and it was ensured that the tips of the electrodes were in contact with the pia on the entire flat of the array before the impulse. After this, the array was covered with saline irrigated surgical cotton strips and left to settle.

The array's pedestal was fixed to a piece of exposed skull using small screws otherwise used in the clinical setting for cranioplasty.

The reference wires were placed securely under the dura. Grounding was achieved either by the pedestal, which is firmly connected to the skull by screws, or by a strong connection to the Mayfield clamp.

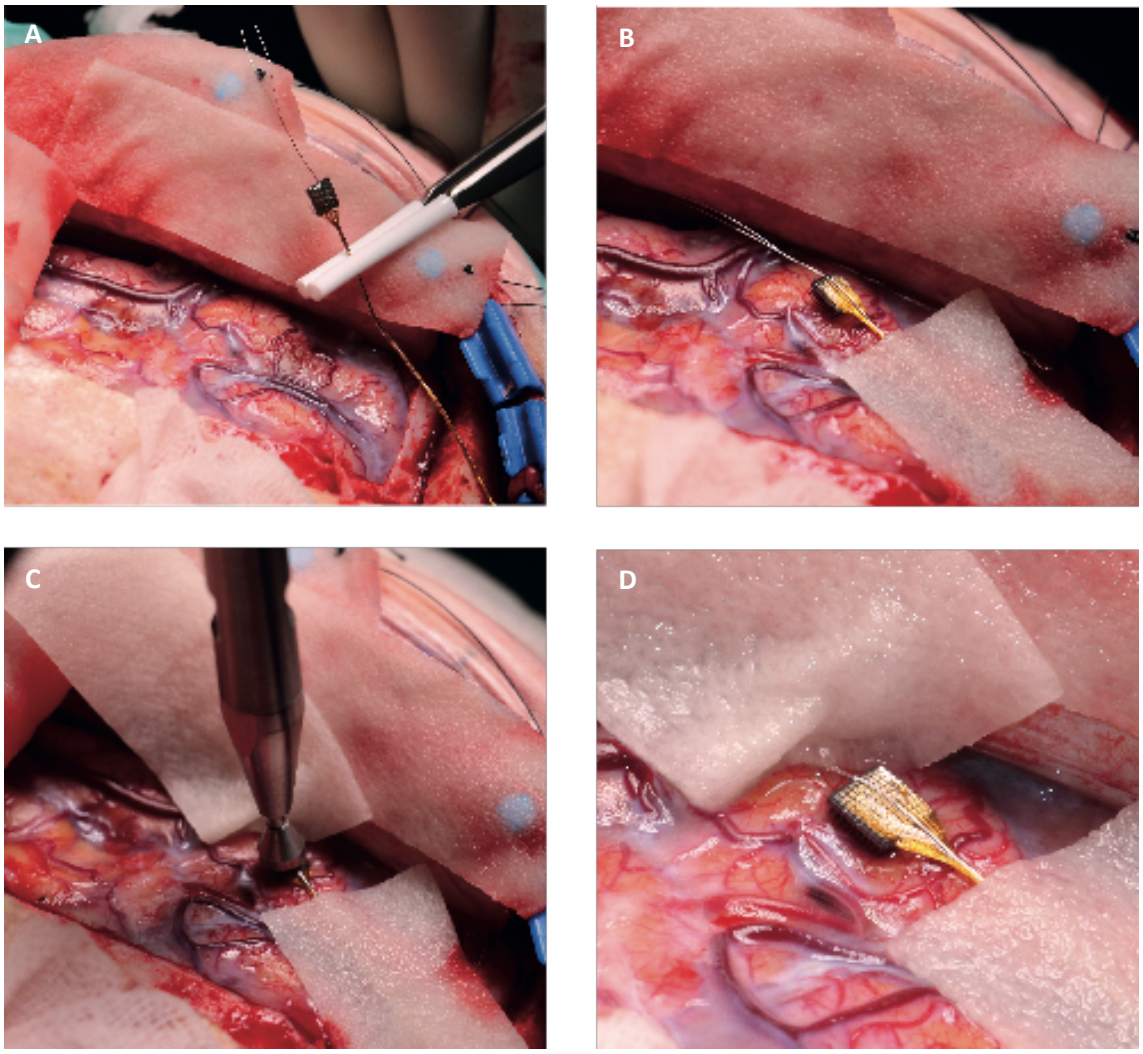

Figure 7. *Intraoperative implantation.* ***A*** *Electrode array before implantation.* ***B*** *Electrode array gently laid on cerebral cortex.* ***C*** *Implantation with pneumatic inserter wand.* ***D*** *Inserted MEA.*

After this step was completed, the supply of anesthetics was reduced to allow the patient to wake up gently. After a wake-up period of varying duration and extubation of the patient, either clinically required testing like cortical stimulation mapping was performed or we began with a slow introduction to the formerly practiced task. The hand switch was placed in the previously determined hand of the now fully awakened subject. The patients then performed the task for between 20 and 30 minutes until either patient exhaustion or the minimum number of 200 trials were reached, while at the same time the extracellular neuronal signals were recorded on all channels of a 25 or 96-channel electrode. Hereafter, the electrode and pedestal were explanted, and resection of the tumor was done, which did not differ from tumor resection in the awake state outside of our study. In three participants (P01-P03), the resected implantation region war formalin-fixed with the arrays in situ and processed further for histological analysis (hematoxylin eosin staining).

During the entire time the patient was awake in the operating room, the subject was supervised by a neuropsychologist in addition to the surgical and anesthesiologic personnel.

2.6 Spike sorting

The waveform separation was performed offline. For manual spike sorting we used the continuously recorded data files with the above-mentioned preset filter settings.

As a first step, we applied an additional digital Highpass filter, a 250Hz Bessel (4^{th} order) filter, to the signal on all channels. Spike sorting was then mainly principal component analysis (PCA) based. In some cases, this did not lead to the desired quality in the sorting process, so feature analysis such as spike width or height was used. Spike sorting was done with the *Plexon Offline Sorter* (Plexon Inc., Dallas, USA).

2.7 Analysis of the LFPs

All analysis of the LFP signal was performed using the raw signal recorded at a sampling rate of 30kHz. The following two analog filters were always applied by our setup: 0.3 Hz Butterworth (1^{st} order) Highpass filter, 7.5kHz Butterworth (3^{rd} order) lowpass filter. The analysis of the LFP signal was mostly done with the *FieldTrip* toolbox (Oostenveld, Fries et al. 2011). Further analysis was made using custom-written Matlab algorithm.

2.7.1 Preprocessing

The LFPs were cut into trials based on the codes (time stamps) sent by the behavioral software. Hereby, each activity of the subjects could be exactly assigned to a time point within the neuronal data. We applied data-padding with additional 1s segments at the beginning and end of each trial. This helps to allow spectral sliding-window analysis at low frequencies. Any eventual line noise artifacts were eliminated by applying a narrow (0.6 Hz width) Butterworth filter (4^{th} order) at 50, 100 and 150 Hz.

2.7.2 Spectral transformation

The spectral transformation was based on previous work (Jacob, Hahnke et al. 2018).

We computed the complex time-frequency representations X of single LFP trials by convolution of signal x with complex kernels k:

$$X(t,\omega) = x(t) * k(t,\omega)$$

where t is time and ω is frequency, $*$ is the convolution operator and k are the frequency-dependent Hanning-tapered complex sinusoids:

$$k(t,\omega) = A\left(1 - \cos\left(\frac{2\pi t\omega}{q}\right)\right)e^{2i\pi t\omega}$$

where A is a constant normalizing k to unit power and the kernel width (number of cycles) is represented by q. Frequencies ranged from 2 to 256, spaced logarithmically in steps of $2^{1/8}$, and kernel widths of 3 were used.

2.7.3 Power

Time varying power pow_x of signal x at frequency ω was estimated as the squared norm of its time-frequency transformation:

$$pow_x(t,\omega) = |X(t,\omega)|^2$$

Additionally, the power was averaged across, trials, sessions and electrodes. It was also z-scored to baseline, the 500ms pre-sample period:

$$z_{pow_x}(t,\omega) = \frac{pow_x(t,\omega) - \mu_{BL}(\omega)}{S_{BL}(\omega)}$$

where $\mu_{BL}(\omega)$ is the mean and $S_{BL}(\omega)$ is the standard deviation of $pow_x(t,\omega)$ during the baseline period at frequency ω.

2.7.4 Spike triggered average of the LFP

The spike-triggered average of the local field potential can be described as the value of the LFP around the spike occurrence as a function of time. This is averaged over all spikes assigned to a given unit. The electrodes were divided into three groups to highlight differences in the three-dimensional propagation of the neuronal signal: the “reference electrode” (the electrode on which the spikes were recorded), and one group each with contacts that were more or less than one millimeter away from the reference electrode in the array setup.

3 Results

The goal of my thesis was to prove it feasible to perform hyperacute intracortical extracellular recordings with multi-electrode arrays of different association cortices in the setting of a medically indicated awake craniotomy. In addition, we wanted to show that this could be combined with the successful performance of a task.

3.1 Successfully completion of working memory task during AC

The phase immediately following awakening from general anesthesia varies greatly between and even within individuals. Thus, it was unclear how a group of patients who are currently in the awake stage of their brain tumor resection with various physical and psychological challenges would perform in a working memory task. As mentioned, the patients were introduced to the task the day before their surgery for around 20 minutes.

All six patients completed the delayed match-to-sample task, four of whom showed an acceptable result under all conditions and two of whom (P07 and P09) failed to exceed the chance-level on the non-symbolic trials. These were excluded from further analyses.

The overall performance in the training session was significantly above chance level and deteriorated only slightly during the surgery ($p = 0.04$, one tailed t test; Fig 8A). The response time increased nonsignificantly during the surgery ($p = 0.23$, one-tailed t test per participant; $p < 0.001$, one-tailed Wilcoxon test with pooled trials; Fig 8B). A response window of one second can therefore be considered long enough for such a test.

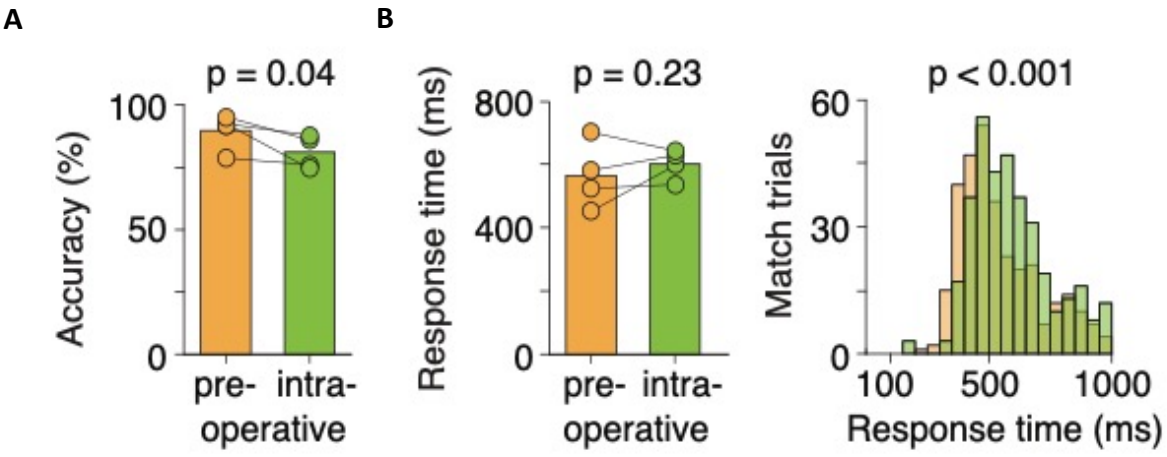

Figure 8. *Pre- and intraoperative cognitive performance of patients undergoing awake brain surgery* ***A*** *pre- and intraoperative task performance (n=4 participants, one-tailed t test)* ***B*** *Pre- and intraoperative response times in match trials on a per-participant basis (left) and pooled across trials (right) (one-tailed t tests).*

Another remarkable effect under the described circumstances was that the patients were able to maintain a high accuracy in their answers after a short “habituation phase” (Fig 9). Due to interindividual differences, each recording session took different amounts of time, but each patient completed between 200 and 300 trials. Patients not being able to concentrate after a certain amount of time or similar effects expected by some did not occur.

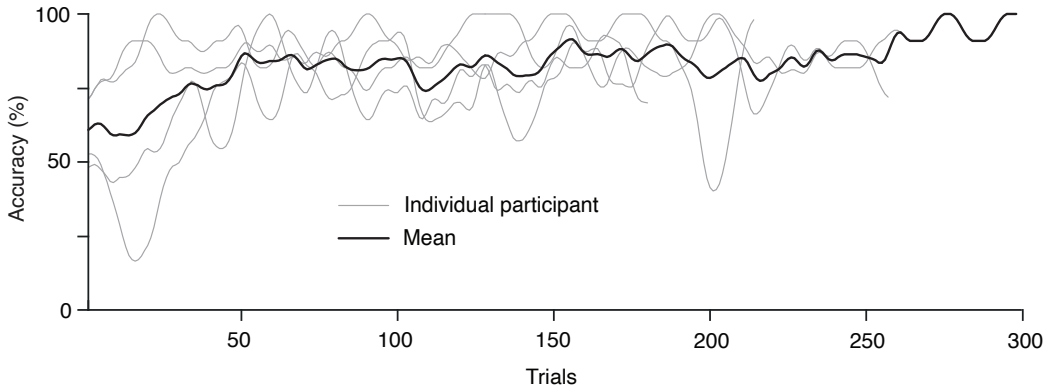

Figure 9. *Time course of patient performance across sessions*

Further analyzing the behavior, the pre- and intraoperative performance continued to be very similar. We showed that the patients were able to correctly match sample and test stimuli in both match and non-match trials (Fig 10C and D, peak of each curve). As the difficulty level increased with increasing numbers, a decrease in accuracy was apparent. In addition, we observed in non-match trials that the rate of error was also higher when the numerical distance of the test from the sample was larger (Fig 10A and B). This effect was larger in non-symbolic trials, which corresponds to observations, which were already determined in similar experiments with non-human primates (Nieder 2003).

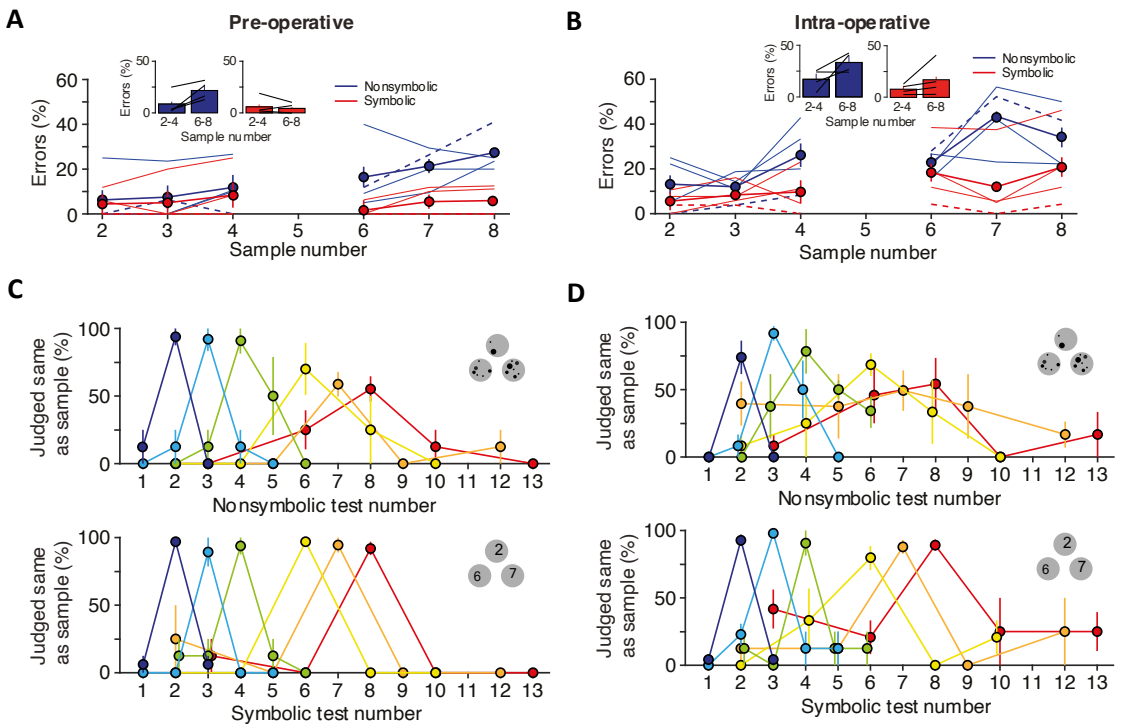

Figure 10. *Comparison of the pre- and intraoperative behavioral data of the patients.* ***A*** *Percentage of errors during preoperative behavioral testing, plotted as a function of sample number and stimulus notation. Inset: performance pooled across small numbers (2–4) and large numbers (6–8). Error bars indicate SEM across participants. Dashed lines mark single-subject data for P10.* ***B*** *Same layout as in A for intraoperative testing.* ***C*** *Preoperative behavioral tuning functions for trials with numbers presented in nonsymbolic and symbolic notation (top and bottom, respectively). Performance is shown for all sample-test-combinations. The peak of each curve represents the percentage of correct match trials, and other data points mark the percentage of errors in non-match trials. Error bars indicate SEM across participants.* ***D*** *Same layout as in C for intraoperative testing*

3.1.1 Example of deviation: acalculia

One patient showed clear deviation from the otherwise displayed behavior during training and surgery (Fig 11; P07). This subject gave the correct answer in 88% of the symbolic trials compared to 22% in nonsymbolic trials. This was later interpreted as acalculia. The backgrounds of such complex disorders could be related to the simultaneously measured neuronal activity und thus better understood. However, we focused on patients who performed acceptably under both conditions in the current evaluation.

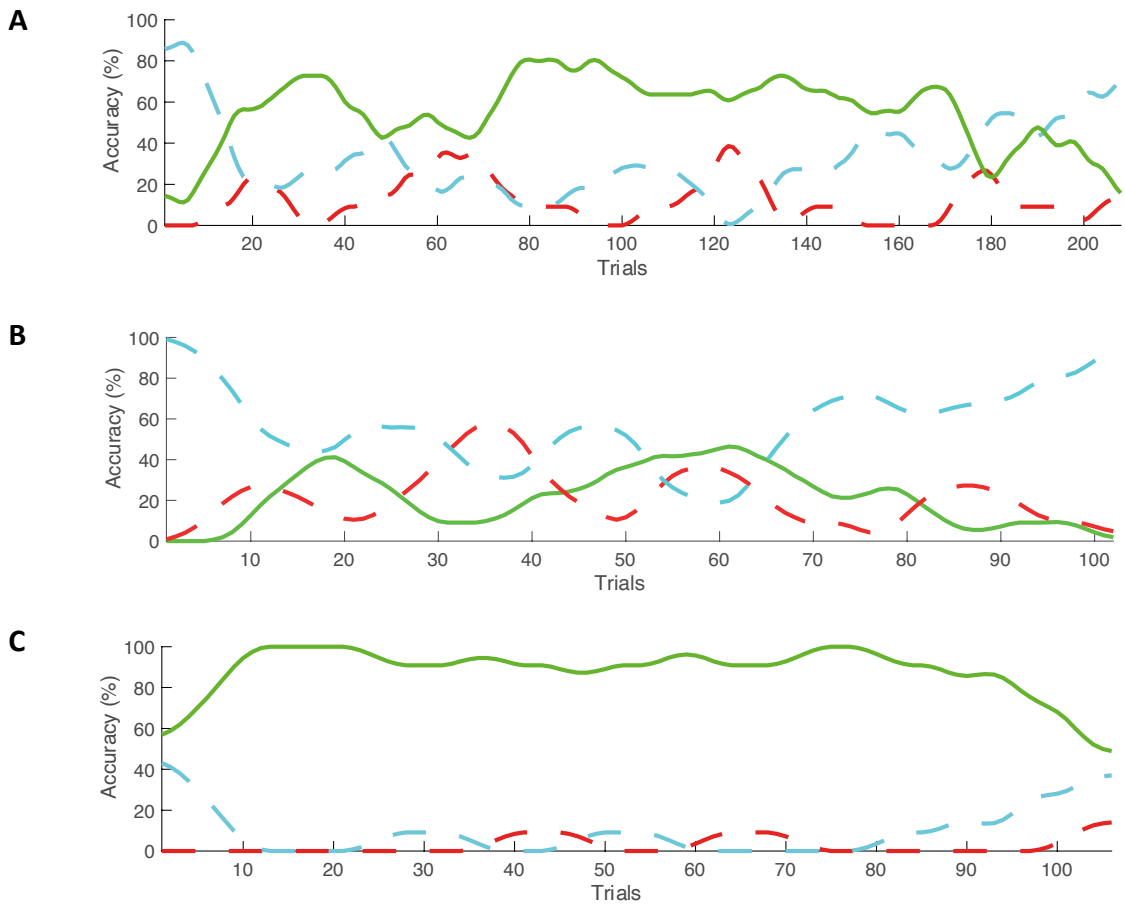

Figure 11. *Representation of the averaged performance during a training session (in bins of 11 trials) of a patient with acalculia. The colors show the proportion of correct (green), incorrect (red) and missed answers (cyan). Trials in which the patient released the button before the test was presented were eliminated.* ***A*** *Performance during entire training session across all trial types. 55% of trials correct.* ***B*** *Performance in nonsymbolic trials. 22% of trials correct.* ***C*** *Performance in symbolic trials. 88% of trials correct.*

3.2 Broad cortical access

Electrophysiological recordings in awake humans are often limited to certain brain regions due to ethical reasons. This is typically the case with epilepsy surgery (temporal lobe) or DBS implantation (globus pallidus internus, thalamus, subthalamic nucleus and pedunculopontine nucleus). Some questions that can only be answered to a limited extent in the animal model can therefore not be transferred to humans. The potential offered by everyday clinical practice could be increasingly used for experimental purposes. This also includes open access to cerebral structures during neurosurgical interventions such as tumor resections.

3.2.1 Reaching a large part of the left hemisphere during awake surgery

The awake brain surgery represents one of the very rare situations in which one has free access to the brain surface of an awake human. This opportunity arising in large supra-regional medical centers can be increasingly exploited through new scientific approaches. However, awake brain surgery must be strictly indicated, and not all interventions and patients are suitable. In our medical center, Department of neurosurgery of *Klinikum rechts der Isar of TU Munich*, Germany, awake surgery is mostly indicated for resection of tumors that are close to brain regions that are relevant for speech, since speech is one of the functions that, unlike motor or sensory functions for example, cannot be monitored in the anesthetized state. From this follows that only left hemispheric space-occupying lesions were included.

To investigate which brain regions are accessible via this procedure, imaging data from awake craniotomies performed at our department from September 2016 until December 2020 were analyzed (Fig 12). Re-resections and patients, who did not receive adequate post-operative imaging at our institution were excluded from the analysis.

Our results show that many areas on the left cerebral convexity can be examined in awake tumor resections.

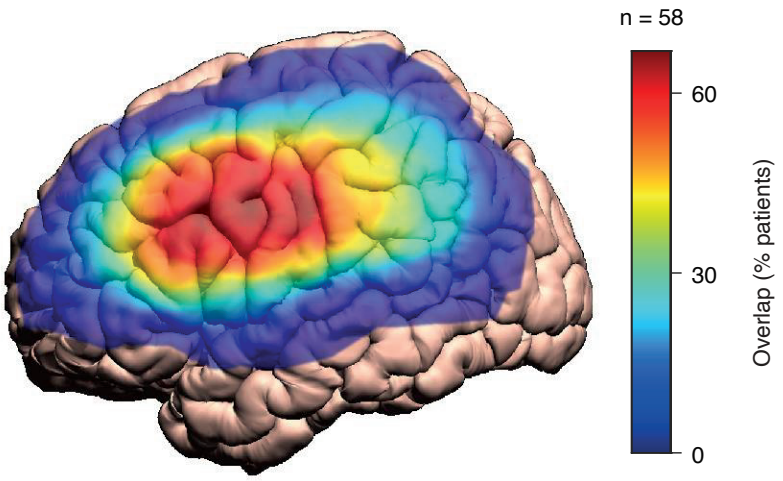

Figure 12. *Craniotomies of n=58 awake resections of brain tumors were transferred to the International Consortium for Brain Mapping (ICBM) template brain surface. Regions with strong overlaps are highlighted in red. Overlays were smoothed with a 2-D Gaussian smoothing kernel with standard deviation of 7.*

3.3 Low damage at insertion site

Three of the implantation sites were histologically analyzed. For this purpose, tumor resections in the anesthetized state were selected. A 96-channel electrode array was implanted in the surgical access route, so no additional damage was caused by removing a block of brain tissue measuring a few millimeters. The puncture channels left behind could be traced in part from the pia mater entry site to the electrode tip (Fig 13A). Thus, an exact analysis of the damage caused as well as the depth of entry could be carried out.

Histopathology demonstrated that deeper cortical layers were reached. In two of three participants, no structural abnormalities were seen in the area of the implanted electrode array. In one, very small microhemorrhages, i.e., microbleedings, were detected in the area of some electrode shafts (Fig 13B). These were limited to the entry canal and had no space-occupying effect. It must be noted that these effects occurred in very close proximity to the trauma caused by the insertion of the electrode array and that there was no evidence of structural consequences at greater distances.

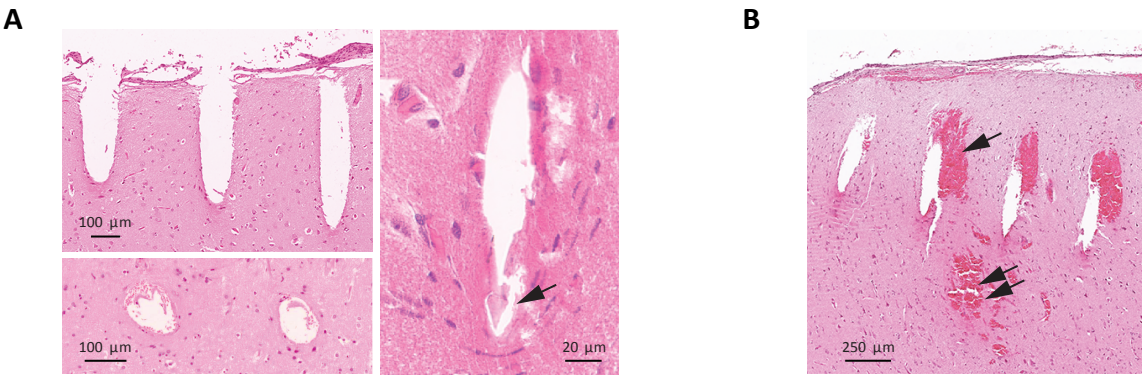

Figure 13. *Histological analysis of example implantation sites.* ***A*** *Histological sections of an example implantation site, showing electrode tracts as they penetrate the pia mater (top left, longitudinal section), along the electrode shaft (bottom left, axial section), and at the electrode tip (right, arrow).* ***B*** *Histological section of a different implantation site showing microhemorrhages along the electrode tracts (single arrow) and in deeper cortical layers (double arrow). See also Table S1.*

3.4 Temperature of the exposed cortical surface decreases only slightly during tumor resection

The temperature of neuronal tissue influences its activity (Robertson and Money 2012). Since the cortical surface is exposed during a craniotomy and could thus be subject to cooling during the course of the experiment, the temperature of the exposed cortex was measured. A high-resolution infrared camera was used during speech mapping and recording of neuronal signals with our experimental setup during an awake tumor resection (Fig 14). The brain surface remained structurally intact, so that

the results are comparable to the time period of recordings with an implanted electrode array and the processing of a task by the patient before tumor resection. Only a cooling down to a minimum of 34.5° C after 15 minutes was detected (Fig 14B). The temperature did not drop further but remained rather constant (Fig 14C). Hereby, we could exclude the influence of time and thus of cortex temperature on the results of our electrophysiological measurements.

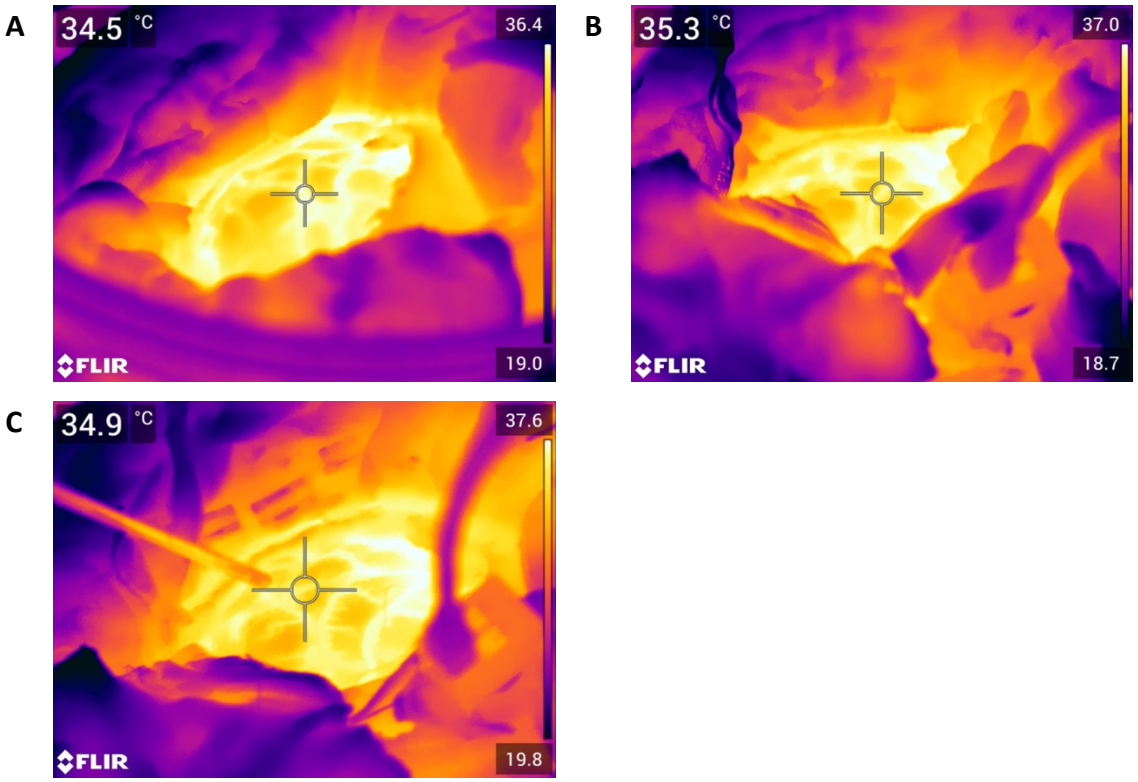

Figure 14. *Temperature of the cortical surface during the first 90 minutes after craniotomy. The number in the upper left corner shows the temperature in the area of the crosshair.* ***A*** *Temperature 15 minutes after performing craniotomy.* ***B*** *Temperature about one hour after performing craniotomy. On the lower edge of the picture, a Cereplex E headstage is visible, attached to the pedestal of an electrode array that was implanted in the interim.* ***C*** *Temperature about 90 minutes after performing craniotomy. A surgical suction device approaches the brain from the left edge of the image.*

3.5 Stable wide-band extracellular recordings during awake craniotomy

Neuronal signals were recorded from the time of the implantation of the array. This signal was composed of local field potentials (LFPs) and single unit spiking activity. Since these recordings did not take place under laboratory conditions, it was necessary to constantly counteract newly occurring problems and disturbances.

3.5.1 Local field potentials

As previously described, the electrode array can be used to measure LFPs. Since this signal can be derived constantly, it is susceptible to interference. During one recording, the electrode responsible for the ground was placed between the patient's eyebrows, which led to significant interference of the signal by saccadic eye movement (Fig 15). As this poor placement of the ground can easily be avoided, this problem is effortless to fix. If such a problem only becomes apparent during subsequent inspection of the data, it can be eliminated by elaborate post-recording analysis.

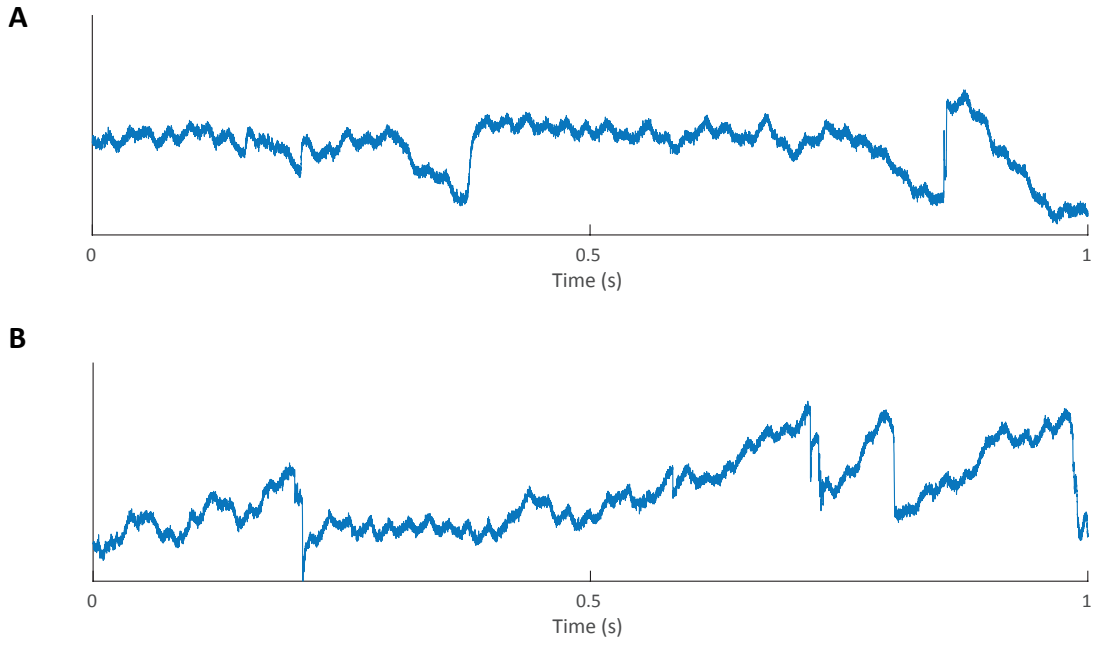

Figure 15. *Two unfiltered example 30kHz LFP traces with interference by saccadic eye movement.* ***A*** *One exemplary second of the LFP trace in anesthetized state. Besides disturbances caused by eye movements, oscillations in low frequencies are depicted.* ***B*** *Similar interferences are also recorded in the awake state.*

The satisfactory quality of the neuronal signals in connection with the successful completion of the task by the subject allows a common analysis of LFPs. For this purpose, we conducted sliding window spectral decomposition that quantifies the power of different frequency bands. This can be done, for example, for each individual electrode for each individual trial (Fig 16) or one averages over electrodes or trials or sessions to identify suspected patterns in the signals.

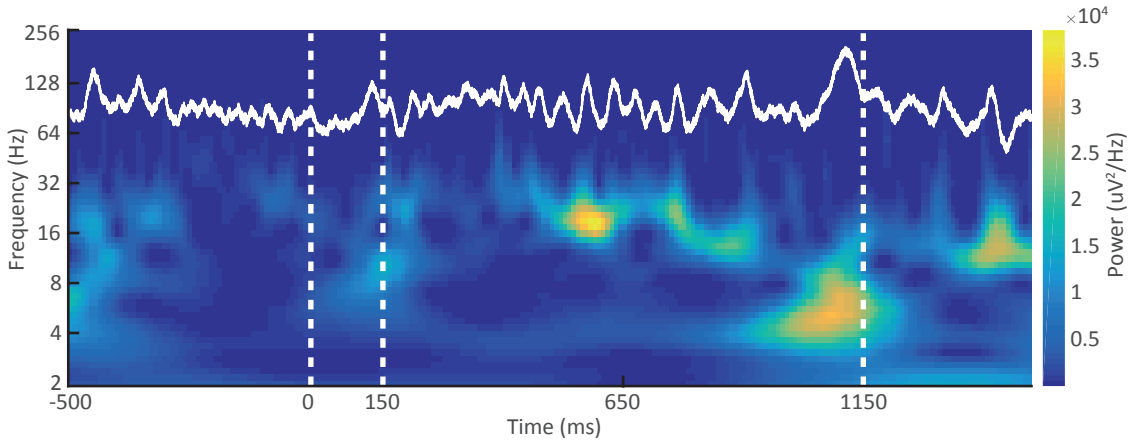

Figure 16. *Sliding window spectral decomposition quantifying the power of distinct frequency bands in one single exemplary trial; white line: high-pass filtered LFP trace. Dotted lines mark beginning and ending of the sample presentation and the end of the memory period.*

A closer look is worthwhile at the different network activity when processing nonsymbolic and symbolic trials (Fig 17). Differences in the power of different frequency bands in the course of the trial can be uncovered. In the individual, a distinct change in activity at the beta-band directly after the stimulus presentation and towards the end of the memory period were observed (Fig. 17A).

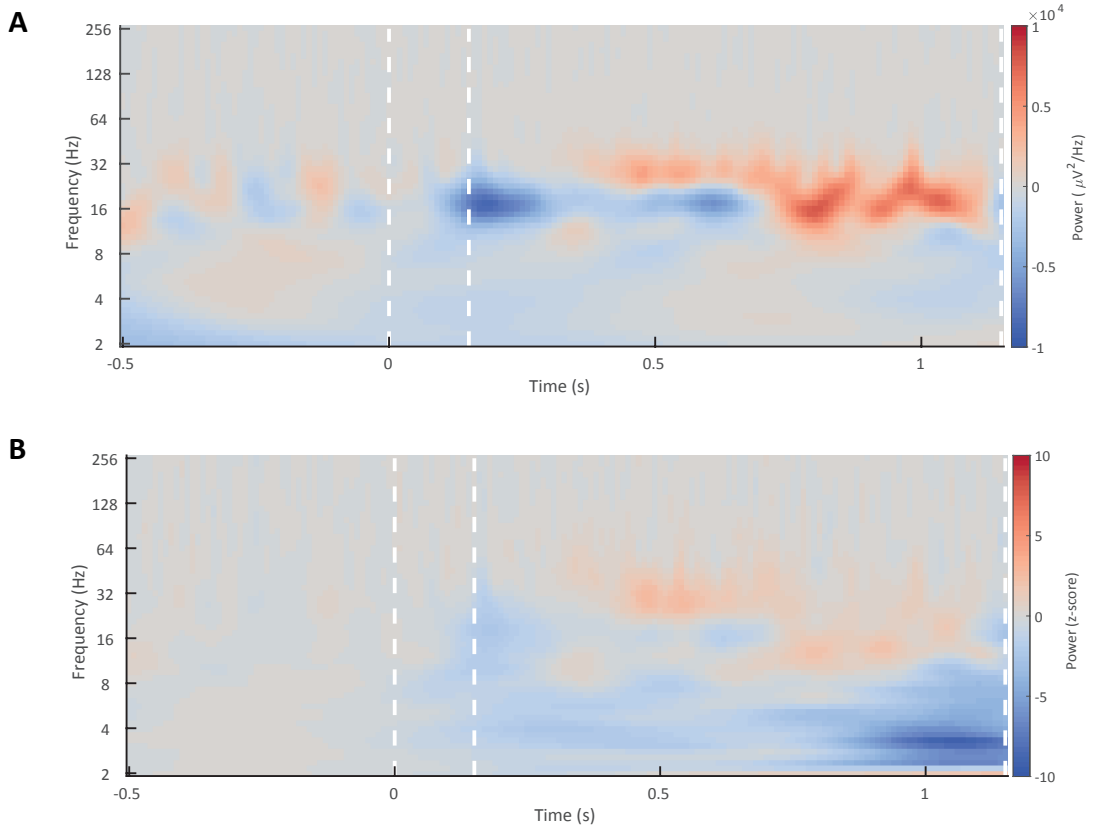

Figure 17. *Sliding window spectral decomposition quantifying the power of distinct frequency bands. Difference of the mean over all nonsymbolic trials on all channels and the mean of all symbolic trials on all channels of one patient (P06). Dotted lines mark beginning and ending of the sample presentation and the end of the memory period.* ***A*** *Power in μV²/Hz.* ***B*** *Power baselined to the 500ms pre-sample period.*

3.5.2 Extraction of action potentials as single- and multi-unit activity

The recording quality was good enough to investigate not only the temporally and spatially summed signals as local field potentials. It was also possible to extract a varying number of single- or multi-unit activity (see Table 1). If the signal-to-noise ratio was sufficient, some of these events triggered by action potentials could already be detected with the eye in the high-pass filtered traces (Fig 18). Since the distance between the contacts is 400 µm, this activity can be described as independent unit activity, which means that the electrical activity of one single neuron cannot be recorded on two different electrodes at the same time.

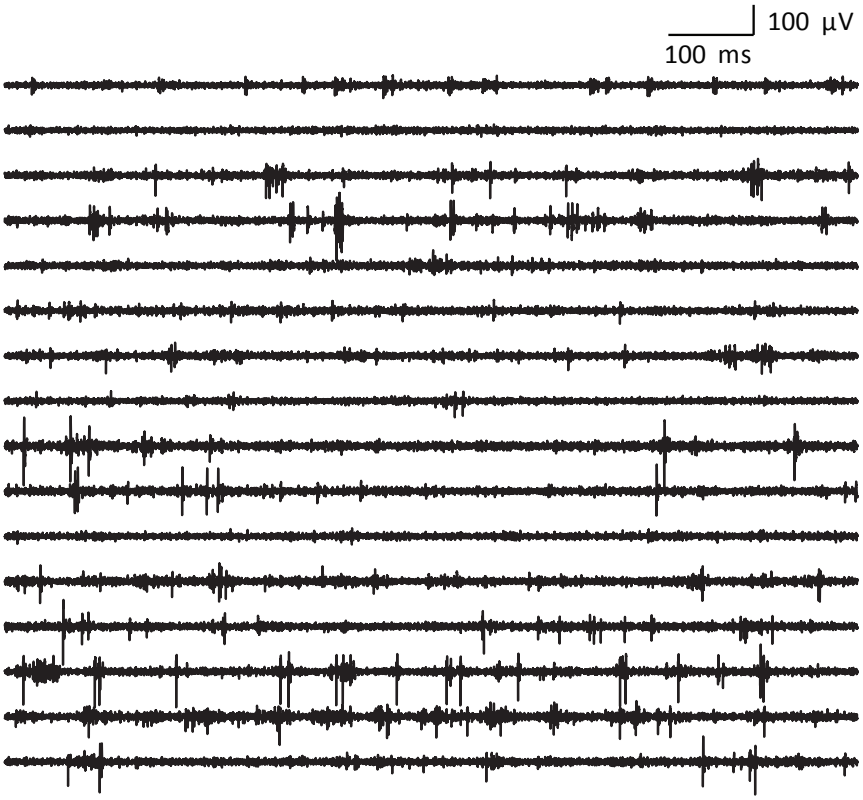

Figure 18. *Exemplary section of the high-pass filtered spiking activity of all 25 channels of a 25-channel array (P10; 1s traces)*

Several methods exist to extract this unit activity from the raw data. The manual sorting method is only successful for a certain signal-to-noise ratio and was carried out according to usual procedures, i.e., including PCA. Distinct waveform clusters representing isolated single units were separated from noise (Fig 19A, B and C, same recording as Fig 18, P10). Following this procedure, single units could be isolated on most electrodes in the example lower-density electrode array (Fig 20A).

A frequency of at least 1Hz during the entire recording, i.e., one spike per second, was defined as the limit for the inclusion of individual units in further analyses.

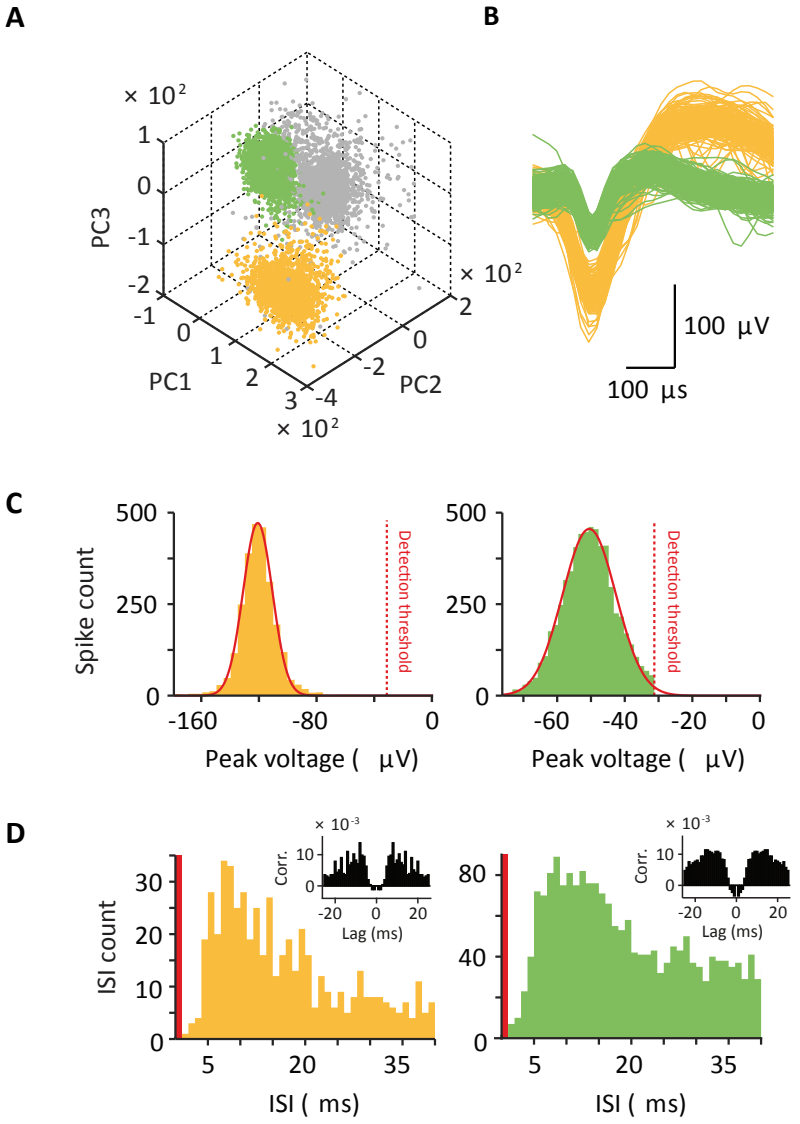

Figure 19. *Isolation of single units from intraoperative recordings.* ***A*** *Principal-component decomposition of thresholded waveforms recorded on an individual channel, showing two distinct waveform clusters (yellow and green) separated from noise (gray).* ***B*** *Waveforms of the single units isolated by principal-component analysis (PCA) in* ***A****.* ***C*** *Distribution of waveform negative peak (trough) voltages for the two example units with Gaussian fits and the selected detection threshold.* ***D*** *Distribution of inter-spike-intervals (ISIs) for the two example units together with spike train autocorrelograms (insets). The refractory period (ISI < 1 ms) is marked in red.*

Across all analyzed recordings, single units were rarely picked up by the higher-density arrays (2% of channels) but frequently isolated on the lower-density arrays (62% of channels; $p < 0.001$, Fisher's exact test, higher-density vs. lower-density arrays; Fig 20B). The first units appeared usually after a few minutes.

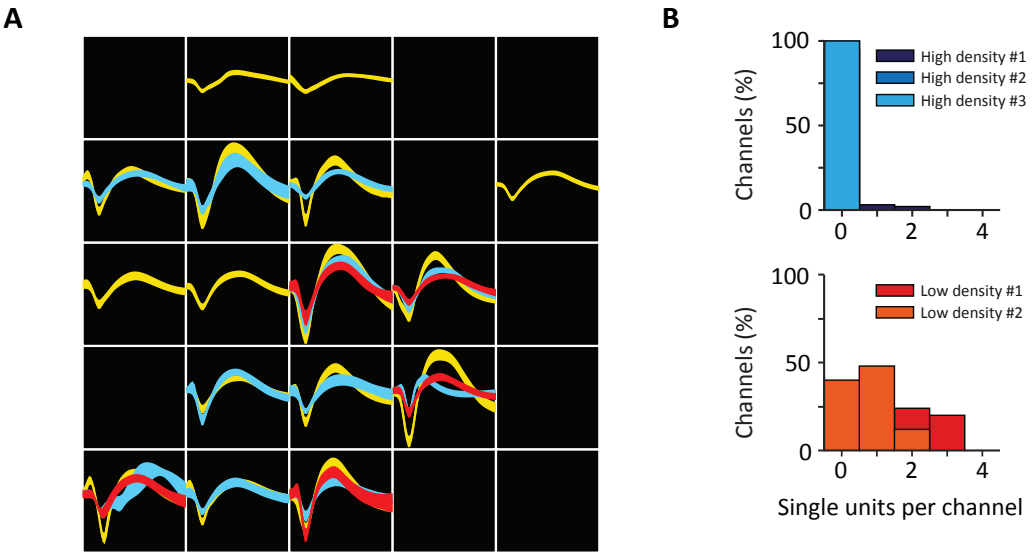

Figure 20. *Single Units from intraoperative recordings.* ***A*** *Average single-unit waveforms recorded from a lower-density MEA. Bands indicate standard deviation across waveforms. Channels with multiunit activity but no well-isolated single units are black.* ***B*** *Distribution of channels with well-isolated activity of one or more single unit(s) recorded from higher-density and lower-density arrays (top and bottom, respectively).*

3.6 Exploiting the two-dimensional structure of the electrode array

One of the biggest advantages of the Utah electrode array is its fixed 2-dimensional design. In the 96-channel version, each independent tip is exactly 400 micrometers away from the horizontally adjacent tips. The advantage of the clear assignment of electrode and anatomical location can be used for further analyses. To measure the effect of a location with spiking activity on postsynaptic activity at another location, the spike triggered average was recorded (Einevoll, Kayser et al. 2013). Two examples of this are shown below (Fig 21), where the limitation of the spread of the activity of the spiking unit could be shown.

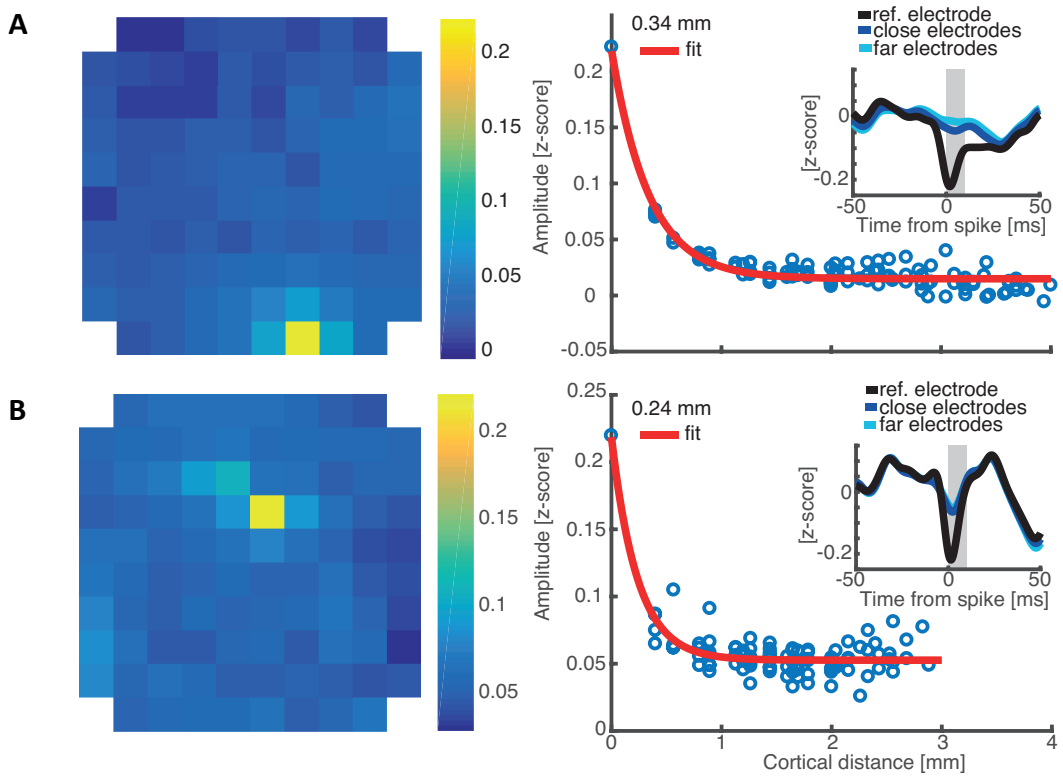

Figure 21. *Effect of a location with spiking activity on postsynaptic activity at another location. Example for two single units from one recording. Z-scored amplitude of the LFP at the moment of the spike until 10ms afterwards (gray shaded area in the right graphs). Close electrodes had a distance to the reference electrode that was less than 1mm, far electrodes were further away than 1mm. Inlet of the right graphs: average amplitude in these two groups. The number above the legend for the fit describes the slope of the function.* ***A*** *Trial-averaged LFP amplitudes triggered on spiking activity on reference channel (10,7).* ***B*** *Trial-averaged LFP amplitudes triggered on spiking activity on reference channel (4,6).*

3.7. Coding of nonsymbolic and symbolic numbers

As shown before, it was possible to record single neuron activity in association cortices of human patients engaged in a working memory task with symbolic and nonsymbolic number.

Previous work has shown that individual neurons of the non-human primate frontoparietal cortex prefer specific numbers (i.e. they are tuned to numerosity) and therefore contribute to number encoding abilities (Nieder, Diester et al. 2006, Jacob and Nieder 2014, Jacob, Hahnke et al. 2018). Recently, neurons in human inferior posterior parietal cortex have been found that respond to symbolic number (Arabic numerals) (Rutishauser, Aflalo et al. 2018).

Next, the behavior of action potentials of single units in the fronto-parietal association cortex during the processing of our task was investigated in more detail.

Using data from an exemplary patient (P10) with the MEA implanted in the IPL, further read-outs are demonstrated in the following:

During trials with representation of non-symbolic number, an exemplary single unit showed significantly increased activity immediately after presentation of the sample stimulus (Fig 22A, left). This increase war strongest for 7 and 8 dots. A similar effect was seen in trials with symbolic numbers, but to a lesser extent (Fig 22A, right).

From this it can be concluded that this specific unit carried information regarding both numerosity and notation (ω^2 percent explained variance, Fig 22C). A cell with similar responses could be detected on an adjacent electrode in this session (Fig 22D-F).

A multi-unit tuned to lower numerosities could be isolated on a different channel in the same session (Fig 22G-I). In trials with symbolic representation of number, however, the firing rate corresponded more to a categorical representation of lower and higher number (Fig 22H and I).

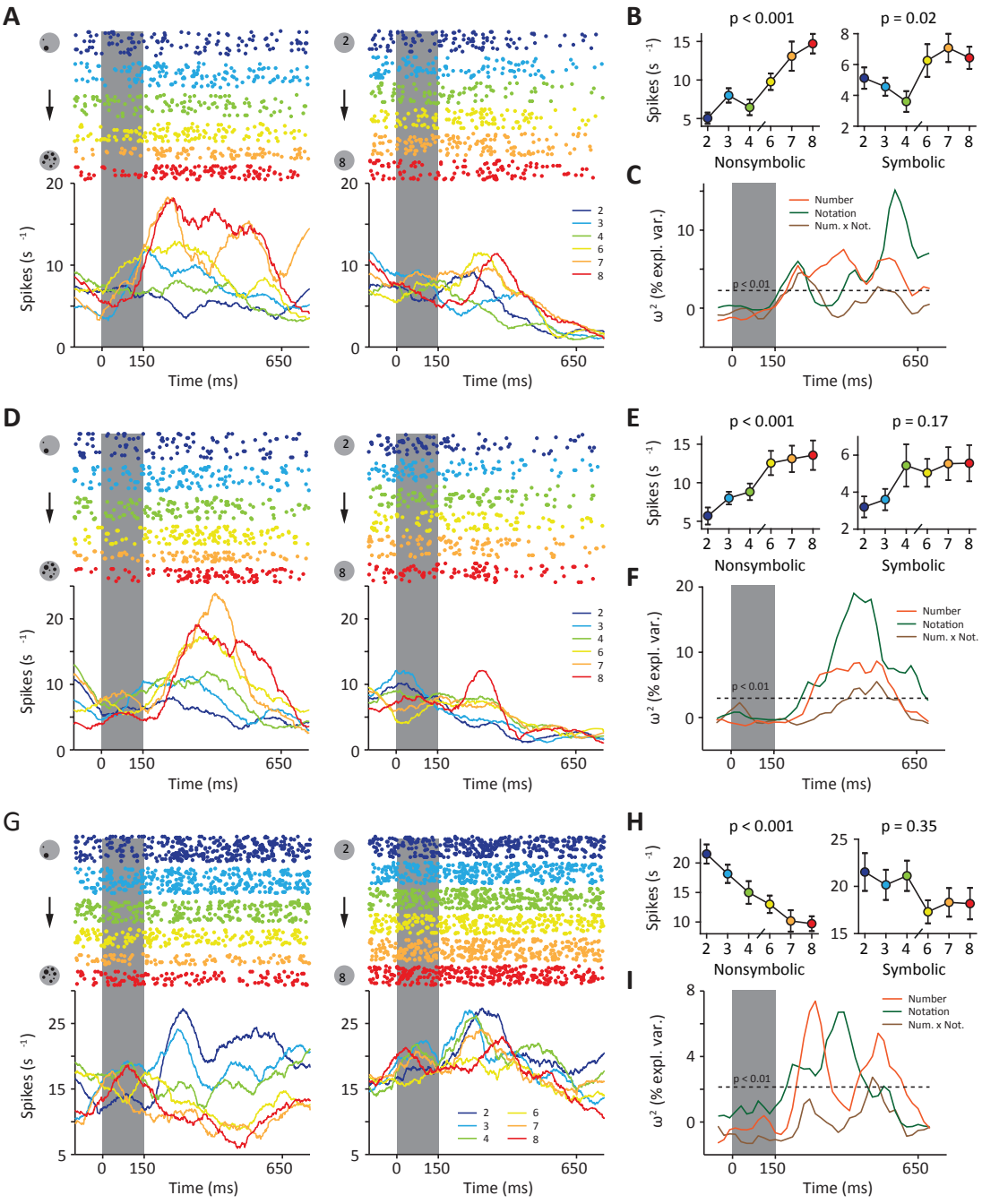

Figure 22. *Single-unit coding of nonsymbolic and symbolic numbers.*

A *Spike raster plots and spike-density histograms (smoothed using a 150-ms Gaussian window) for an example single unit recorded in the inferior parietal lobe. Trials are sorted by sample numerosity and by stimulus notation (left, nonsymbolic; right, symbolic). Sample presentation is highlighted.* ***B*** *Firing rate of the neuron in A in the 500-ms epoch following presentation of nonsymbolic and symbolic sample numerosities (left and right, respectively; one- factorial ANOVA). Error bars indicate SEM across trials.* ***C*** *Sliding-window u2 percent explained variance (two-factorial ANOVA) quantifying the information about sample number and notation as well as their inter- action contained in the firing rate of the neuron in A in correct trials. A dashed line marks the significance threshold (p = 0.01, shuffle distribution).* ***D–F*** *Same layout as in A–C for a different single units recorded on a neighboring channel on the same MEA.* ***G–I*** *Same layout as in A–C for a multiunit recorded on a neighboring channel on the same MEA.*

4 Discussion

Electrophysiological recordings of brain activity have a fundamental role on the road to a better understanding of higher brain functions in humans. There is a multitude of established methods for a wide variety of clinical and scientific applications.

I have shown that intracortically implanted multi-electrode arrays during awake craniotomies represent a feasible and reliable method to robustly record human brain activity with single-cell resolution in the acute setting. Combining intracortical recording of neuronal signals with intraoperative tasks performed by an awake patient opens new perspectives to address specific questions in fundamental neuroscience.

4.1 MEAs in neurosurgical craniotomies – incorporating fundamental science into the operating room

The method described so far has been proven by us to be feasible for use in the clinical setting. The relative simplicity of the application makes it possible to introduce MEA recordings into the operating room without changes in the established neurosurgical procedures and the medically necessary processes at the core. With adequate preoperative planning, the implantation took on average 10 minutes.

Time is a critical factor in modern medicine: from the patient's perspective on the one hand and in the economic context on the other. After initial training of the team, we consider the required time for array implantation acceptable, not causing an unreasonable delay in operation routines.

Apart from the pneumatic inserter wand, no electrode holder or manipulator is needed, which leads to an accelerated insertion process. Importantly, it allows free access to a wide area of cortical tissue of the surgical site during further neurosurgical intervention, which can be seen is as a major advantage compared to other methods such as, for example, the neuropixels probe (Paulk, A.C., Kfir, Y., Nat. Neuroscience 2022), which is a flexible, high-density microelectrode with around 1000 recording sites on a very narrow shank. In various trials, several hundreds of single-units could be recorded (Chung, Sellers et al. 2022)

It must be mentioned that the manual insertion of the array also caused difficulties: due to the lack of mechanical support, it is a challenge to precisely perform the pneumatic array insertion. The array has to be placed flat on the cortex and the inserter again placed flat on the back of the MEA. A short pulse is then used to introduce the electrode tips into the cortex in a controlled manner. Exact alignment is the key here (and may be subject to interindividual differences). Evidently specific demands are placed on the neurosurgical team. Our results suggest that the challenges regarding the implantation can be overcome, and good signal quality can be ensured.

Our setup was installed on a movable cart and thus free to install (and remove) in any operation room needed. The non-necessity of creating special infrastructure in the operating room to establish recordings with MEAs in the clinic leads to easier cooperation between clinicians and scientists and will help to better exploit the existing potential of interventions performed for medical reasons. This will be of even more importance in the future, as it is only through high-volume recordings that we will gain a better understanding of cognitive functions in humans. Since awake craniotomies are generally performed at higher case numbers than, for example, DBS implantations or epilepsy surgery, this underlines the potential of our experimental setup.

Lastly, reproduction of scientific results is essential for the validation of specific findings: The lower the effort, the faster the learning processes and the more straightforward the results are to reproduce.

4.2 Feasibility of performing a task addressing higher human cognitive functions during awake craniotomy

Awake craniotomy offers the unique possibility of direct access to the human cortex in the awake state of a subject. We show that despite the high requirements to perform a working memory task by subjects undergoing awake brain surgery, the performance deteriorates only marginally and within an acceptable range, always remaining clearly above chance-level (Figure 8).

Despite our small sample size, it can also be concluded that the additional burden for patients performing a task during awake craniotomy is acceptable. Interdisciplinary interaction of neurosurgeons, anesthesiologists, operating room nurses, research teams and neuropsychologists is indispensable. In a highly professional team trained for this situation, it is possible to create an adequate atmosphere in which the patient can work on such a task between medically necessary measures, concentrated and almost pain-free. In this regard, there were no complaints postoperatively within our patient cohort. A central aspect when carrying out highly complex experiments in awake patients is pre-operative management: selection of suitable patients and planning of such surgeries, where tact and sensitivity are needed, are decisive for later success.

4.3 MEAs are suitable for acute recordings of human brain activity

MEAs have been a tool used for years to record neuronal activity in various contexts (Davis, Wark et al. 2016, Paulk, Kfir et al. 2022, Durand, Heller et al. 2023). We were able to show that good signal quality can be achieved in the acute setting during tumor resections. Compared to existing alternatives as the neuropixels probe mentioned above, no further mechanical stabilization is required. The design allows free "floating" on the cortex. When using linear probes for example, the slight shifts of the skull or the pulsation of the brain, which inevitably occur in living objects, pose great challenges for scientists, especially during data analysis. This motion correction is not necessary with the method we use, since the MEA follows the natural as unnatural movements of the brain, e.g., when manipulating near the implanted electrode array.

In addition, the material used has a complete safety profile established through many years of use. Everything except the electrode arrays itself can be reused or sterilized, which reduces costs and makes this type of research more sustainable.

Another advantage of the used experimental setup, which is crucial for approval by the ethics committee, is patient safety which can be ensured by lack of risk of shank breakage. The "loss" of materials introduced into the body for research purposes is virtually impossible with conscientious use, since all components are always visible.

Another major point that makes the use of MEAs advantageous is broad cortical access. Evaluation of awake craniotomies from a single center shows that this method can be used to reach many brain areas in awake craniotomies (Figure 12). Limitations known from recordings during DBS implantations or epilepsy surgery do not apply here which increases the application possibilities and the frequency of use.

No piotomies or corticotomies are needed to implant the MEA, which reduces damage to functional brain tissue and the time of situs exposed during surgery, which consequently also reduces the risk of infection.

It was also shown that the signal quality was robust at a good level with single unit resolution (Fig 19) and analyzable low-pass filtered LFP data (Fig 16). Grounding was achieved either by the pedestal, which is firmly connected to the skull by screws, or by a strong connection to the Mayfield clamp. Both options achieved a satisfactory reduction of hum and noise, resulting in an elevated signal-to-noise ratio and high-quality recordings with single-cell resolution. It must be noted that the setting is very different from laboratory conditions. In the operating room are many electrical devices producing interfering signals and noise. Switching off any of the equipment that is standard in a modern operating room, be it lights, suction, warming blankets, hemostatic instruments, surgical microscopes or large wall screens and cameras for neuronavigation, was not necessary.

4.4 Grid-like electrode arrangement

The grid-like arrangement of the MEA used in the experiments is one of its strongest features. It allows dense sampling of neuronal activity in the horizontal plane. The activity of neighboring neurons and a network on the microcircuit scale in the target region can be investigated in detail. This can be used to serve the increased interest in propagating neuronal activity, e.g., in form analyses of travelling waves (Muller, Chavane et al. 2018). Competing methods, such as microwire bundles or linear probes, are less suitable for this purpose. This advantage can be multiplied as several MEAs can be implanted simultaneously in the same patient (Woeppel, Hughes et al. 2021) or combined with ECoG grids. Thus, there are very few limits to spatial coverage.

4.5 Geometric configuration of the MEA is decisive factor of SNR

The geometric configuration of the MEA is unsurprisingly a factor significantly influencing the quality of the recordings. Particularly affected is the SNR of the spiking activity. The version of the Utah array with increased interelectrode spacing (Figure 4) recorded on average one well-isolated single unit per channel. With the unmodified version of the Utah arrays, this could not be achieved. However, good LFP signals were found with both.

Especially in the hyperacute setting of awake craniotomies this factor comes to the fore. The increased interelectrode distance reduces the trauma to the region of implantation. That trauma occurs has been suggested by our histological analyses, as microhemorrhages could be detected in some but not all channels left by the electrode tips (Figure 13). Nonetheless, the extent of the trauma was limited and did not cause complete loss of function or severe distortion of the electrical activity of the recorded cells in the target region.

With both array versions, LFPs could be recorded immediately in good quality, but single-unit activity appeared only after a few minutes and the quality of the signals improved until the start of data recording. Since MEA implantation was performed in an anesthetized state and the patient had to be awakened afterwards anyways in order to adequately perform the tasks required for safe tumor resection, no time was lost. Even though these few minutes until appearance of single unit activity seem to be longer than recently reported for thinner linear probes (Chung, Sellers et al. 2022, Paulk, Kfir et al. 2022), this is not a compelling argument against our method given the significantly shorter implantation time.

The modified arrays with increased interelectrode distance were implanted in the last 4 patients of our cohort. We see no evidence that the improvement of the recordings could be explained by growing experience of the surgical team. The significant increase in unit activity described in the results (Figure

19B) did not occur gradually, but abruptly after introducing the Utah arrays with increased interelectrode space.

4.6 Combination of in vivo with in vitro experiments

In our experimental setup, the cortex block in which the MEA was implanted was resected during surgery. This opens up the possibility of postoperative continuation of the analyses on the removed brain tissue. In particular, this could include the histological workup with exact determination of the cytoarchitecture of the brain region as well as electrophysiological experiments in vitro.

4.7 Ethical issues and experimental limitations

The raised questions cannot be investigated in an animal model. For ethical reasons, the MEAs were only implanted in areas of the brain that were resected anyway for the purpose of tumor resection. Additional damage caused by the implantation can thus be ruled out.

However, following this, the electrophysiological data are limited to be recorded from regions that are potentially histopathologically altered.

Although no standard for maintaining a safety margin around the tumor was established, thorough preoperative and intraoperative planning using MRI-guided neuronavigation and the long experience of the neurosurgical team in inspecting the anatomical conditions ensured that implantation was performed in healthy tissue surrounding the tumor. This was confirmed by the histopathological analyses of some implantation sites in which no tumor infiltration was seen (Figure 13).

Additionally, the recordings are limited to a few millimeters below the brain surface, the cortex. Deeper brain regions are inaccessible to MEAs.

Due to the indication of awake craniotomies for monitoring speech practiced in our medical center, the tumors and consequently the implantation sites were limited to the left hemisphere of the brain. Since these surgeries are performed regularly but not daily, and due to further prerequisites for our research such as sufficient German language skills of the patients or the completeness of the involved scientific and clinical team, the sample size has been small so far. With growing experience and sufficient staff training, some of these obstacles can be overcome easily.

Nevertheless, the sample size is large enough to demonstrate the scientifically valuable application of implantation of MEAs in awake craniotomies, recording good signals also on a single cell level in combination with a behavioral task involving higher mental functions.

At a time when brain computer interfaces (BCI) are becoming increasingly important, this method can be a powerful addition to the armentarium of neuroscience in order to better understand the unique processes of the human brain.

5 References

Agrillo, C., L. Piffer and A. Bisazza (2011). "Number versus continuous quantity in numerosity judgments by fish." Cognition **119**(2): 281-287.

Andreas Nieder, D. J. F., Earl K. Miller (2002). "Representation of the Quantity of Visual Items in the Primate
Prefrontal Cortex." Science.

Arrighi, R., I. Togoli and D. C. Burr (2014). "A generalized sense of number." Proc Biol Sci **281**(1797).

Asaad, W. F. and E. N. Eskandar (2008). "A flexible software tool for temporally-precise behavioral control in Matlab." J Neurosci Methods **174**(2): 245-258.

Baddeley, A. (1992). "Working memory." Science **255**(5044): 556-559.

Baddeley, A. (2012). "Working memory: theories, models, and controversies." Annu Rev Psychol **63**: 1-29.

Balakhonov, D. and J. Rose (2017). "Crows Rival Monkeys in Cognitive Capacity." Sci Rep **7**(1): 8809.

Brown, T., A. H. Shah, A. Bregy, N. H. Shah, M. Thambuswamy, E. Barbarite, T. Fuhrman and R. J. Komotar (2013). "Awake craniotomy for brain tumor resection: the rule rather than the exception?" J Neurosurg Anesthesiol **25**(3): 240-247.

Bu, J., K. D. Young, W. Hong, R. Ma, H. Song, Y. Wang, W. Zhang, M. Hampson, T. Hendler and X. Zhang (2019). "Effect of deactivation of activity patterns related to smoking cue reactivity on nicotine addiction." Brain **142**(6): 1827-1841.

Buschman, T. J., M. Siegel, J. E. Roy and E. K. Miller (2011). "Neural substrates of cognitive capacity limitations." Proc Natl Acad Sci U S A **108**(27): 11252-11255.

Buzsaki, G., C. A. Anastassiou and C. Koch (2012). "The origin of extracellular fields and currents--EEG, ECoG, LFP and spikes." Nat Rev Neurosci **13**(6): 407-420.

Chacko, A. G., S. G. Thomas, K. S. Babu, R. T. Daniel, G. Chacko, K. Prabhu, V. Cherian and G. Korula (2013). "Awake craniotomy and electrophysiological mapping for eloquent area tumours." Clin Neurol Neurosurg **115**(3): 329-334.

Chao, L. L. and R. T. Knight (1995). "Human prefrontal lesions increase distractibility to irrelevant sensory inputs." Neuroreport **6**(12): 1605-1610.

Chao, L. L. and R. T. Knight (1998). "Contribution of human prefrontal cortex to delay performance." J Cogn Neurosci **10**(2): 167-177.

Chatham, C. H. and D. Badre (2015). "Multiple gates on working memory." Curr Opin Behav Sci **1**: 23-31.

Chung, J. E., K. K. Sellers, M. K. Leonard, L. Gwilliams, D. Xu, M. E. Dougherty, V. Kharazia, S. L. Metzger, M. Welkenhuysen, B. Dutta and E. F. Chang (2022). "High-density single-unit human cortical recordings using the Neuropixels probe." Neuron **110**(15): 2409-2421 e2403.

Collee, E., A. Vincent, C. Dirven and D. Satoer (2022). "Speech and Language Errors during Awake Brain Surgery and Postoperative Language Outcome in Glioma Patients: A Systematic Review." Cancers (Basel) **14**(21).

Constantinidis, C. and M. A. Steinmetz (1996). "Neuronal activity in posterior parietal area 7a during the delay periods of a spatial memory task." J Neurophysiol **76**(2): 1352-1355.

Cowan, N. (2001). "The magical number 4 in short-term memory: a reconsideration of mental storage capacity." Behav Brain Sci **24**(1): 87-114; discussion 114-185.

Cowan, N. (2017). "The many faces of working memory and short-term storage." Psychon Bull Rev **24**(4): 1158-1170.

Curtis, C. E. and M. D'Esposito (2003). "Persistent activity in the prefrontal cortex during working memory." Trends Cogn Sci **7**(9): 415-423.

Daume, J., T. Gruber, A. K. Engel and U. Friese (2017). "Phase-Amplitude Coupling and Long-Range Phase Synchronization Reveal Frontotemporal Interactions during Visual Working Memory." J Neurosci **37**(2): 313-322.

Davis, T. S., H. A. Wark, D. T. Hutchinson, D. J. Warren, K. O'Neill, T. Scheinblum, G. A. Clark, R. A. Normann and B. Greger (2016). "Restoring motor control and sensory feedback in people with upper extremity amputations using arrays of 96 microelectrodes implanted in the median and ulnar nerves." J Neural Eng **13**(3): 036001.

Dehaene, S., G. Dehaene-Lambertz and L. Cohen (1998). "Abstract representations of numbers in the animal and human brain." Trends Neurosci **21**(8): 355-361.

Deuschl, G., C. Schade-Brittinger, P. Krack, J. Volkmann, H. Schafer, K. Botzel, C. Daniels, A. Deutschlander, U. Dillmann, W. Eisner, D. Gruber, W. Hamel, J. Herzog, R. Hilker, S. Klebe, M. Kloss, J. Koy, M. Krause, A. Kupsch, D. Lorenz, S. Lorenzl, H. M. Mehdorn, J. R. Moringlane, W. Oertel, M. O. Pinsker, H. Reichmann, A. Reuss, G. H. Schneider, A. Schnitzler, U. Steude, V. Sturm, L. Timmermann, V. Tronnier, T. Trottenberg, L. Wojtecki, E. Wolf, W. Poewe, J. Voges and N. S. German Parkinson Study Group (2006). "A randomized trial of deep-brain stimulation for Parkinson's disease." N Engl J Med **355**(9): 896-908.

Durand, S., G. R. Heller, T. K. Ramirez, J. A. Luviano, A. Williford, D. T. Sullivan, A. J. Cahoon, C. Farrell, P. A. Groblewski, C. Bennett, J. H. Siegle and S. R. Olsen (2023). "Acute head-fixed recordings in awake mice with multiple Neuropixels probes." Nat Protoc **18**(2): 424-457.

Eger, E., V. Michel, B. Thirion, A. Amadon, S. Dehaene and A. Kleinschmidt (2009). "Deciphering cortical number coding from human brain activity patterns." Curr Biol **19**(19): 1608-1615.

Einevoll, G. T., C. Kayser, N. K. Logothetis and S. Panzeri (2013). "Modelling and analysis of local field potentials for studying the function of cortical circuits." Nat Rev Neurosci **14**(11): 770-785.

Eisenkolb, V. M., L. M. Held, A. Utzschmid, X. X. Lin, S. M. Krieg, B. Meyer, J. Gempt and S. N. Jacob (2023). "Human acute microelectrode array recordings with broad cortical access, single-unit resolution, and parallel behavioral monitoring." Cell Rep **42**(5): 112467.

Emrich, S. M., A. C. Riggall, J. J. Larocque and B. R. Postle (2013). "Distributed patterns of activity in sensory cortex reflect the precision of multiple items maintained in visual short-term memory." J Neurosci **33**(15): 6516-6523.

Ester, E. F., J. T. Serences and E. Awh (2009). "Spatially global representations in human primary visual cortex during working memory maintenance." J Neurosci **29**(48): 15258-15265.

Feredoes, E., K. Heinen, N. Weiskopf, C. Ruff and J. Driver (2011). "Causal evidence for frontal involvement in memory target maintenance by posterior brain areas during distracter interference of visual working memory." Proc Natl Acad Sci U S A **108**(42): 17510-17515.

Fias, W., J. Lammertyn, B. Reynvoet, P. Dupont and G. A. Orban (2003). "Parietal representation of symbolic and nonsymbolic magnitude." J Cogn Neurosci **15**(1): 47-56.

Funahashi, S., C. J. Bruce and P. S. Goldman-Rakic (1989). "Mnemonic coding of visual space in the monkey's dorsolateral prefrontal cortex." J Neurophysiol **61**(2): 331-349.

Fuster, J. M. and G. E. Alexander (1971). "Neuron activity related to short-term memory." Science **173**(3997): 652-654.

Gerritsen, J. K. W., M. L. D. Broekman, S. De Vleeschouwer, P. Schucht, C. Jungk, S. M. Krieg, B. V. Nahed, M. S. Berger and A. Vincent (2022). "Global comparison of awake and asleep mapping procedures in glioma surgery: An international multicenter survey." Neurooncol Pract **9**(2): 123-132.

Glover, G. H. (2011). "Overview of functional magnetic resonance imaging." Neurosurg Clin N Am **22**(2): 133-139, vii.

Gottlieb, Y., E. Vaadia and M. Abeles (1989). "Single unit activity in the auditory cortex of a monkey performing a short term memory task." Exp Brain Res **74**(1): 139-148.

Gross, H. J., M. Pahl, A. Si, H. Zhu, J. Tautz and S. Zhang (2009). "Number-based visual generalisation in the honeybee." PLoS One **4**(1): e4263.

Habib, S. H. and S. S. Habib (2021). "Auditory brainstem response: An overview of neurophysiological implications and clinical applications -A Narrative Review." J Pak Med Assoc **71**(9): 2230-2236.

Hajat, Z., N. Ahmad and J. Andrzejowski (2017). "The role and limitations of EEG-based depth of anaesthesia monitoring in theatres and intensive care." Anaesthesia **72 Suppl 1**: 38-47.

Herreras, O. (2016). "Local Field Potentials: Myths and Misunderstandings." Front Neural Circuits **10**: 101.

Hill, N. J., D. Gupta, P. Brunner, A. Gunduz, M. A. Adamo, A. Ritaccio and G. Schalk (2012). "Recording human electrocorticographic (ECoG) signals for neuroscientific research and real-time functional cortical mapping." J Vis Exp(64).

Hochberg, L. R., D. Bacher, B. Jarosiewicz, N. Y. Masse, J. D. Simeral, J. Vogel, S. Haddadin, J. Liu, S. S. Cash, P. van der Smagt and J. P. Donoghue (2012). "Reach and grasp by people with tetraplegia using a neurally controlled robotic arm." Nature **485**(7398): 372-375.

Honkanen, R., S. Rouhinen, S. H. Wang, J. M. Palva and S. Palva (2015). "Gamma Oscillations Underlie the Maintenance of Feature-Specific Information and the Contents of Visual Working Memory." Cereb Cortex **25**(10): 3788-3801.

Hwang, J., A. R. Mitz and E. A. Murray (2019). "NIMH MonkeyLogic: Behavioral control and data acquisition in MATLAB." J Neurosci Methods **323**: 13-21.

Jacob, S. N., D. Hahnke and A. Nieder (2018). "Structuring of Abstract Working Memory Content by Fronto-parietal Synchrony in Primate Cortex." Neuron **99**(3): 588-597 e585.

Jacob, S. N. and A. Nieder (2014). "Complementary roles for primate frontal and parietal cortex in guarding working memory from distractor stimuli." Neuron **83**(1): 226-237.

Jung, R. and W. Berger (1979). "[Fiftieth anniversary of Hans Berger's publication of the electroencephalogram. His first records in 1924--1931 (author's transl)]." Arch Psychiatr Nervenkr (1970) **227**(4): 279-300.

Kaiju, T., K. Doi, M. Yokota, K. Watanabe, M. Inoue, H. Ando, K. Takahashi, F. Yoshida, M. Hirata and T. Suzuki (2017). "High Spatiotemporal Resolution ECoG Recording of Somatosensory Evoked Potentials with Flexible Micro-Electrode Arrays." Front Neural Circuits **11**: 20.

Katrin Amunts, H. M., Sebastian Bludau, Karl Zilles (2020). "Julich-Brain: A 3D probabilistic atlas of the human brain's cytoarchitecture." Science **Vol. 369**(Issue 6506).

Kutter, E. F., J. Bostroem, C. E. Elger, F. Mormann and A. Nieder (2018). "Single Neurons in the Human Brain Encode Numbers." Neuron **100**(3): 753-761 e754.

Lara, A. H., S. W. Kennerley and J. D. Wallis (2009). "Encoding of gustatory working memory by orbitofrontal neurons." J Neurosci **29**(3): 765-774.

Lara, A. H. and J. D. Wallis (2015). "The Role of Prefrontal Cortex in Working Memory: A Mini Review." Front Syst Neurosci **9**: 173.

Lennert, T. and J. Martinez-Trujillo (2011). "Strength of response suppression to distracter stimuli determines attentional-filtering performance in primate prefrontal neurons." Neuron **70**(1): 141-152.

Liebe, S., G. M. Hoerzer, N. K. Logothetis and G. Rainer (2012). "Theta coupling between V4 and prefrontal cortex predicts visual short-term memory performance." Nat Neurosci **15**(3): 456-462, S451-452.

Liem, L. K., J. M. Simard, Y. Song and K. Tewari (1995). "The patch clamp technique." Neurosurgery **36**(2): 382-392.

Linden, H., T. Tetzlaff, T. C. Potjans, K. H. Pettersen, S. Grun, M. Diesmann and G. T. Einevoll (2011). "Modeling the spatial reach of the LFP." Neuron **72**(5): 859-872.

Logothetis, N. K. (2008). "What we can do and what we cannot do with fMRI." Nature **453**(7197): 869-878.

Luck, S. J. and E. K. Vogel (1997). "The capacity of visual working memory for features and conjunctions." Nature **390**(6657): 279-281.

Lundqvist, M., J. Rose, P. Herman, S. L. Brincat, T. J. Buschman and E. K. Miller (2016). "Gamma and Beta Bursts Underlie Working Memory." Neuron **90**(1): 152-164.

Lyons, I. M., D. Ansari and S. L. Beilock (2015). "Qualitatively different coding of symbolic and nonsymbolic numbers in the human brain." Hum Brain Mapp **36**(2): 475-488.

Mayberg, H. S., A. M. Lozano, V. Voon, H. E. McNeely, D. Seminowicz, C. Hamani, J. M. Schwalb and S. H. Kennedy (2005). "Deep brain stimulation for treatment-resistant depression." Neuron **45**(5): 651-660.

Maynard, E. M., C. T. Nordhausen and R. A. Normann (1997). "The Utah intracortical Electrode Array: a recording structure for potential brain-computer interfaces." Electroencephalogr Clin Neurophysiol **102**(3): 228-239.

Mazziotta, J., A. Toga, A. Evans, P. Fox, J. Lancaster, K. Zilles, R. Woods, T. Paus, G. Simpson, B. Pike, C. Holmes, L. Collins, P. Thompson, D. MacDonald, M. Iacoboni, T. Schormann, K. Amunts, N. Palomero-Gallagher, S. Geyer, L. Parsons, K. Narr, N. Kabani, G. Le Goualher, D. Boomsma, T. Cannon, R. Kawashima and B. Mazoyer (2001). "A probabilistic atlas and reference system for the human brain: International Consortium for Brain Mapping (ICBM)." Philos Trans R Soc Lond B Biol Sci **356**(1412): 1293-1322.

Miller, E. K. and J. D. Cohen (2001). "An integrative theory of prefrontal cortex function." Annu Rev Neurosci **24**: 167-202.

Miller, E. K., C. A. Erickson and R. Desimone (1996). "Neural mechanisms of visual working memory in prefrontal cortex of the macaque." J Neurosci **16**(16): 5154-5167.

Miller, E. K., L. Li and R. Desimone (1993). "Activity of neurons in anterior inferior temporal cortex during a short-term memory task." J Neurosci **13**(4): 1460-1478.

Miller, E. K., M. Lundqvist and A. M. Bastos (2018). "Working Memory 2.0." Neuron **100**(2): 463-475.

Miller, K. J., D. Hermes and N. P. Staff (2020). "The current state of electrocorticography-based brain-computer interfaces." Neurosurg Focus **49**(1): E2.

Muller, L., F. Chavane, J. Reynolds and T. J. Sejnowski (2018). "Cortical travelling waves: mechanisms and computational principles." Nat Rev Neurosci **19**(5): 255-268.

Musk, E. and Neuralink (2019). "An Integrated Brain-Machine Interface Platform With Thousands of Channels." J Med Internet Res **21**(10): e16194.

Neher, E. and B. Sakmann (1976). "Single-channel currents recorded from membrane of denervated frog muscle fibres." Nature **260**(5554): 799-802.

Nieder, A. (2016). "The neuronal code for number." Nat Rev Neurosci **17**(6): 366-382.

Nieder, A. and S. Dehaene (2009). "Representation of number in the brain." Annu Rev Neurosci **32**: 185-208.

Nieder, A., I. Diester and O. Tudusciuc (2006). "Temporal and spatial enumeration processes in the primate parietal cortex." Science **313**(5792): 1431-1435.

Nieder, A., D. J. Freedman and E. K. Miller (2002). "Representation of the quantity of visual items in the primate prefrontal cortex." Science **297**(5587): 1708-1711.

Nieder, A. and E. K. Miller (2003). "Coding of cognitive magnitude: compressed scaling of numerical information in the primate prefrontal cortex." Neuron **37**(1): 149-157.

Niedermeyer, E. (1998). "Frontal lobe epilepsy: the next frontier." Clin Electroencephalogr **29**(4): 163-169.

Oostenveld, R., P. Fries, E. Maris and J. M. Schoffelen (2011). "FieldTrip: Open source software for advanced analysis of MEG, EEG, and invasive electrophysiological data." Comput Intell Neurosci **2011**: 156869.

Osorio, I., M. G. Frei, S. Sunderam, J. Giftakis, N. C. Bhavaraju, S. F. Schaffner and S. B. Wilkinson (2005). "Automated seizure abatement in humans using electrical stimulation." Ann Neurol **57**(2): 258-268.

Pasternak, T. and M. W. Greenlee (2005). "Working memory in primate sensory systems." Nat Rev Neurosci **6**(2): 97-107.

Pasternak, T., L. L. Lui and P. M. Spinelli (2015). "Unilateral prefrontal lesions impair memory-guided comparisons of contralateral visual motion." J Neurosci **35**(18): 7095-7105.

Paulk, A. C., Y. Kfir, A. R. Khanna, M. L. Mustroph, E. M. Trautmann, D. J. Soper, S. D. Stavisky, M. Welkenhuysen, B. Dutta, K. V. Shenoy, L. R. Hochberg, R. M. Richardson, Z. M. Williams and S. S. Cash (2022). "Large-scale neural recordings with single neuron resolution using Neuropixels probes in human cortex." Nat Neurosci **25**(2): 252-263.

Pearce, J. M. (2009). "Broca's aphasiacs." Eur Neurol **61**(3): 183-189.

Piazza, M., P. Pinel, D. Le Bihan and S. Dehaene (2007). "A magnitude code common to numerosities and number symbols in human intraparietal cortex." Neuron **53**(2): 293-305.

Postle, B. R. (2006). "Working memory as an emergent property of the mind and brain." Neuroscience **139**(1): 23-38.

R, L. d. N. (1947). "A study of nerve physiology." Stud Rockefeller Inst Med Res Repr **131**: 1-496.

Reif, P. S., A. Strzelczyk and F. Rosenow (2016). "The history of invasive EEG evaluation in epilepsy patients." Seizure **41**: 191-195.

Riggall, A. C. and B. R. Postle (2012). "The relationship between working memory storage and elevated activity as measured with functional magnetic resonance imaging." J Neurosci **32**(38): 12990-12998.

Robertson, R. M. and T. G. Money (2012). "Temperature and neuronal circuit function: compensation, tuning and tolerance." Curr Opin Neurobiol **22**(4): 724-734.

Rutishauser, U., T. Aflalo, E. R. Rosario, N. Pouratian and R. A. Andersen (2018). "Single-Neuron Representation of Memory Strength and Recognition Confidence in Left Human Posterior Parietal Cortex." Neuron **97**(1): 209-220 e203.

Sacko, O., V. Lauwers-Cances, D. Brauge, M. Sesay, A. Brenner and F. E. Roux (2011). "Awake craniotomy vs surgery under general anesthesia for resection of supratentorial lesions." Neurosurgery **68**(5): 1192-1198; discussion 1198-1199.

Salazar, R. F., N. M. Dotson, S. L. Bressler and C. M. Gray (2012). "Content-specific fronto-parietal synchronization during visual working memory." Science **338**(6110): 1097-1100.

Shattuck, D. W. and R. M. Leahy (2002). "BrainSuite: an automated cortical surface identification tool." Med Image Anal **6**(2): 129-142.

Siegler, R. S. and J. E. Opfer (2003). "The development of numerical estimation: evidence for multiple representations of numerical quantity." Psychol Sci **14**(3): 237-243.

Soto, F. A. and E. A. Wasserman (2014). "Mechanisms of object recognition: what we have learned from pigeons." Front Neural Circuits **8**: 122.

Starowicz-Filip, A., K. Prochwicz, A. Myszka, R. Krzyzewski, K. Stachura, A. A. Chrobak, A. M. Rajtar-Zembaty, B. Betkowska-Korpala and B. Kwinta (2022). "Subjective experience, cognitive functioning and trauma level of patients undergoing awake craniotomy due to brain tumor - Preliminary study." Appl Neuropsychol Adult **29**(5): 983-992.

Suzuki, M. and J. Gottlieb (2013). "Distinct neural mechanisms of distractor suppression in the frontal and parietal lobe." Nat Neurosci **16**(1): 98-104.

Viswanathan, P. and A. Nieder (2013). "Neuronal correlates of a visual "sense of number" in primate parietal and prefrontal cortices." Proc Natl Acad Sci U S A **110**(27): 11187-11192.

Wang, Y., X. Yang, X. Zhang, Y. Wang and W. Pei (2023). "Implantable intracortical microelectrodes: reviewing the present with a focus on the future." Microsyst Nanoeng **9**: 7.

Ward, A. A. and L. B. Thomas (1955). "The electrical activity of single units in the cerebral cortex of man." Electroencephalogr Clin Neurophysiol **7**(1): 135-136.

Whalen, J., Gallistel, C. R., & Gelman, R. (1999). "Nonverbal Counting in Humans: The Psychophysics of Number Representation." Psychological Science **10**(2): 130-137.

Willett, F. R., D. T. Avansino, L. R. Hochberg, J. M. Henderson and K. V. Shenoy (2021). "High-performance brain-to-text communication via handwriting." Nature **593**(7858): 249-254.

Willett, F. R., E. M. Kunz, C. Fan, D. T. Avansino, G. H. Wilson, E. Y. Choi, F. Kamdar, M. F. Glasser, L. R. Hochberg, S. Druckmann, K. V. Shenoy and J. M. Henderson (2023). "A high-performance speech neuroprosthesis." Nature **620**(7976): 1031-1036.

Woeppel, K., C. Hughes, A. J. Herrera, J. R. Eles, E. C. Tyler-Kabara, R. A. Gaunt, J. L. Collinger and X. T. Cui (2021). "Explant Analysis of Utah Electrode Arrays Implanted in Human Cortex for Brain-Computer-Interfaces." Front Bioeng Biotechnol **9**: 759711.

Wong, A. K., J. L. Shils, S. B. Sani and R. W. Byrne (2022). "Intraoperative Neuromonitoring." Neurol Clin **40**(2): 375-389.

6. Acknowledgements

First, I would like to thank my supervisor Prof. Dr. Simon Jacob for his exceptional support during the realization of this project and of my scientific and clinical career so far.

I also want to thank Prof. Dr. Meyer, Prof. Dr. Gempt and Prof. Dr. Krieg and the rest of staff for the integration of this research into the highly demanding everyday clinical work at the Department of Neurosurgery of Klinikum rechts der Isar of TU Munich.

For the good cooperation in the publication process of the paper I would like to thank in particular Lisa Held, Alex Utzschmid and Xiaoxiong Lin.

Special thanks to my colleagues of the Jacob Lab, past and present, for the constant support and the fruitful scientific and non-scientific discussions.